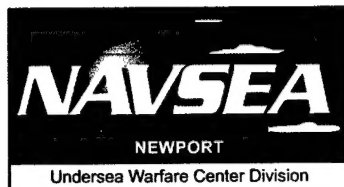


NUWC-NPT Technical Report 11,541
19 April 2004

Detection Performance of a Suboptimum Processor in Non-Gaussian Noise

Albert H. Nuttall
Sensors and Sonar Systems Department



20040615 123

**Naval Undersea Warfare Center Division
Newport, Rhode Island**

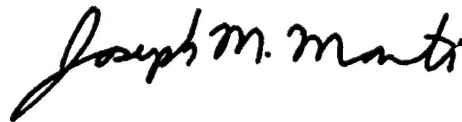
Approved for public release; distribution is unlimited.

PREFACE

The work described in this report was jointly funded under the Naval Undersea Warfare Center's "Large-N Strategic Initiative" project, principal investigator Clifford M. Curtis (Code 152), and the Office of Naval Research's "Large-N Discovery and Invention (D&I)" project, principal investigator Stephen G. Greineder (Code 15221).

The technical reviewer for this report was Michael J. Obara (Code 15221).

Reviewed and Approved: 19 April 2004



Joseph M. Monti
Head, Sensors and Sonar Systems Department



REPORT DOCUMENTATION PAGE

Form Approved
OMB No. 0704-0188

Public reporting for this collection of information is estimated to average 1 hour per response, including the time for reviewing instructions, searching existing data sources, gathering and maintaining the data needed, and completing and reviewing the collection of information. Send comments regarding this burden estimate or any other aspect of this collection of information, including suggestions for reducing this burden, to Washington Headquarters Services, Directorate for Information Operations and Reports, 1215 Jefferson Davis Highway, Suite 1204, Arlington, VA 22202-4302, and to the Office of Management and Budget, Paperwork Reduction Project (0704-0188), Washington, DC 20503.

1. AGENCY USE ONLY (Leave blank)

2. REPORT DATE
19 April 2004

3. REPORT TYPE AND DATES COVERED

4. TITLE AND SUBTITLE

Detection Performance of a Suboptimum Processor in Non-Gaussian Noise

5. FUNDING NUMBERS

6. AUTHOR(S)

Albert H. Nuttall

7. PERFORMING ORGANIZATION NAME(S) AND ADDRESS(ES)

Naval Undersea Warfare Center Division
1176 Howell Street
Newport, RI 02841-1708

8. PERFORMING ORGANIZATION
REPORT NUMBER

TR 11,541

9. SPONSORING/MONITORING AGENCY NAME(S) AND ADDRESS(ES)

Office of Naval Research
Ballston Centre Tower One
800 North Quincy Street
Arlington, VA 22217-5660

10. SPONSORING/MONITORING
AGENCY REPORT NUMBER

11. SUPPLEMENTARY NOTES

12a. DISTRIBUTION/AVAILABILITY STATEMENT

Approved for public release; distribution is unlimited.

12b. DISTRIBUTION CODE

13. ABSTRACT (Maximum 200 words)

The performance of a suboptimum processor for three different signal types in three different noise backgrounds has been investigated numerically in terms of the receiver operating characteristics and compared with the performance of the optimum processor in the same environments. The three distributions considered are Gaussian, sech, and fourth power; the sech distribution decays exponentially for large arguments, while the fourth-power distribution decays inversely proportional to the fourth power. Noise with the fourth-power distribution is very heavy-tailed and constitutes a debilitating effect on standard linear processors in weak signal environments.

The suboptimum processor consists of a hard limiter followed by an energy detector. In the presence of heavy-tailed noise interference, this suboptimum processor approach loses on the order of 1 dB in signal detectability relative to the optimum processor. Lack of the detailed signal structure is not a detriment to this processor; furthermore, the information required to realize the absolute optimum processor will not likely be available in practice.

14. SUBJECT TERMS

Suboptimum Processors
Receiver Operating Characteristics

Energy Detectors
Exponential Noise

Non-Gaussian Noise
Fourth-Power Noise

15. NUMBER OF PAGES
66

16. PRICE CODE

17. SECURITY CLASSIFICATION
OF REPORT
Unclassified

18. SECURITY CLASSIFICATION
OF THIS PAGE
Unclassified

19. SECURITY CLASSIFICATION
OF ABSTRACT
Unclassified

20. LIMITATION OF ABSTRACT
SAR

TABLE OF CONTENTS

	Page
LIST OF ILLUSTRATIONS	ii
LIST OF TABLES	iii
LIST OF ABBREVIATIONS, ACRONYMS, AND SYMBOLS	iii
INTRODUCTION	1
NOISE STATISTICS.....	2
Gaussian Noise.....	2
Sech Noise.....	4
Fourth-Power Noise	8
q Functions for Nonlinearly Transformed Random Variables.....	12
PERFORMANCE OF OPTIMUM PROCESSORS IN NON-GAUSSIAN NOISE.....	20
DERIVATION OF SUBOPTIMUM PROCESSORS	31
PERFORMANCE OF A SUBOPTIMUM PROCESSOR	33
SUMMARY	49
REFERENCES	49
APPENDIX A—INVERSION OF CUMULATIVE DISTRIBUTION FUNCTION FOR FOURTH-POWER RANDOM VARIABLE.....	A-1
APPENDIX B—DEFLECTION CRITERION FOR SUBOPTIMUM PROCESSOR.....	B-1

LIST OF ILLUSTRATIONS

Figure	Page
1 q Functions for Gaussian Noise, $\sigma = 1$	3
2 q Functions for Sech Noise, $\sigma = 1$	6
3 q Functions for Fourth-Power Noise, $\sigma = 1$	10
4 Sample Data Sequences of 1000 Independent Variables	11
5 q Functions for Cubic Transformation, $a = 0.1$, $\sigma_y = 1.32$	14
6 q Functions for Cubic Transformation, $a = 0.2$, $\sigma_y = 1.67$	15
7 q Functions for Cubic Transformation, $a = 0.3$, $\sigma_y = 2.04$	16
8 q Functions for Cubic Transformation, $a = 0.4$, $\sigma_y = 2.41$	17
9 ROCs for Gaussian Signal in Gaussian Noise, Processor G	21
10 ROCs for Gaussian Signal in Sech Noise, Processor G	22
11 ROCs for Gaussian Signal in Fourth-Power Noise, Processor G	23
12 ROCs for Gaussian Signal in Sech Noise, Processor S	25
13 ROCs for Sech Signal in Sech Noise, Processor S	26
14 ROCs for Fourth-Power Signal in Sech Noise, Processor S	27
15 ROCs for Gaussian Signal in Fourth-Power Noise, Processor F	28
16 ROCs for Sech Signal in Fourth-Power Noise, Processor F	29
17 ROCs for Fourth-Power Signal in Fourth-Power Noise, Processor F	30
18 ROCs for Gaussian Signal in Sech Noise, $r = 1.0$	34
19 ROCs for Sech Signal in Sech Noise, $r = 1.0$	35
20 ROCs for Fourth-Power Signal in Sech Noise, $r = 1.0$	36
21 ROCs for Gaussian Signal in Fourth-Power Noise, $r = 0.65$	38
22 ROCs for Sech Signal in Fourth-Power Noise, $r = 0.65$	39
23 ROCs for Fourth-Power Signal in Fourth-Power Noise, $r = 0.65$	40
24 ROCs for Gaussian Signal in Fourth-Power Noise, $r = 0.75$	41
25 ROCs for Gaussian Signal in Fourth-Power Noise, Processor F, $\alpha = -0.5$	43
26 ROCs for Gaussian Signal in Fourth-Power Noise, $r = 0.65$, $\alpha = -0.5$	44
27 ROCs for Gaussian Signal in Fourth-Power Noise, Processor F, $\alpha = 0.0$	45
28 ROCs for Gaussian Signal in Fourth-Power Noise, $r = 0.65$, $\alpha = 0.0$	46
29 ROCs for Gaussian Signal in Fourth-Power Noise, Processor F, $\alpha = [-1, 1]$	47
30 ROCs for Gaussian Signal in Fourth-Power Noise, $r = 0.65$, $\alpha = [-1, 1]$	48
B-1 Program for Deflection Criterion	B-3
B-2 Deflection for Gaussian Noise and Processor (B-6)	B-4
B-3 Deflection for Sech Noise and Processor (B-6)	B-5
B-4 Deflection for Fourth-Power Noise and Processor (B-6)	B-6

LIST OF TABLES

Table		Page
1	Losses of Suboptimum Processor in Sech Noise	33
2	Losses of Suboptimum Processor in Fourth-Power Noise.....	37
3	Dependence of Losses on Signal Structure	42

LIST OF ABBREVIATIONS, ACRONYMS, AND SYMBOLS

a	Positive scale factor, equation (27)
\mathbf{a}_k	Auxiliary random variable, equation (14)
b	Saturation parameter, equations (49) through (51)
c	Cumulative distribution function, equation (10)
\tilde{c}	Inverse cumulative distribution function, equation (23)
$c(u, \lambda)$	c -function, equation (9)
CDF	Cumulative distribution function
CF	Characteristic function
\mathbf{d}_k	Sample value of direct path signal component, equation (44)
E	Ensemble average, appendix B
f	Nonlinear transformation, equations (27) and (34)
\tilde{f}, F	Inverse function to f , equations (27) and (28)
g	Inverse function to f , equation (34)
HT	Heavy tailed
k	Sample number, equations (1) and (44)
K	Number of data samples, equation (1)
L	Likelihood ratio, equation (1)
m	Signal delay, equation (44)
MGF	Moment-generating function
OP	Operating point
$p, p(x)$	Probability density function of noise, equation (1)
p_x	Probability density function of random variable \mathbf{x} , equation (25)
p_y	Probability density function of random variable \mathbf{y} , equations (30) and (31)
PDF	Probability density function
P_d	Probability of detection
P_f	Probability of false alarm
$p_n(u)$	PDF of sum of n sech RVs, equation (17)
q	$\log p$, equations (1) and (2)
q', q''	Derivatives of q function, equation (2)
r	Ratio of saturation value to standard deviation, equation (52)
ROC	Receiver operating characteristic

LIST OF ABBREVIATIONS, ACRONYMS, AND SYMBOLS (Cont'd)

RV	Random variable
\mathbf{s}_k	Signal sample, equation (44)
SNR	Signal-to-noise ratio
$t(y)$	Auxiliary variable, equation (28)
U	Auxiliary variable, equation (18)
v	Probability density function interval, appendix B
\mathbf{x}	Auxiliary random variable, equation (26)
\mathbf{x}_k	Sample k of input data, equation (1)
x_n	Sample argument, equation (42)
\mathbf{w}_k	Auxiliary random variable, equation (51)
\mathbf{y}	Nonlinearly transformed random variable, equations (26) and (48)
y_n	Sample transformed variable, equation (42)
\mathbf{z}_k	Auxiliary random variable, equation (50)
α	Relative attenuation factor, equation (44)
ρ_{kj}	Element of normalized signal covariance matrix, equation (1)
σ	Standard deviation of noise
μ	Moment generating function, equation (6)
χ	Cumulants, equation (8)

DETECTION PERFORMANCE OF A SUBOPTIMUM PROCESSOR IN NON-GAUSSIAN NOISE

INTRODUCTION

The optimum processor for detection of a weak, zero-mean stationary signal in stationary non-Gaussian noise was presented in reference 1. If $p(x)$ is the first-order probability density function (PDF) of the independent input noise background samples, and $q(x) = \log p(x)$, then the optimum processor for low input signal-to-noise ratio (SNR) takes the form

$$\mathbf{L} = \sum_{k=1}^K q''(\mathbf{x}_k) + \sum_{k,j=1}^K \rho_{kj} q'(\mathbf{x}_k) q'(\mathbf{x}_j), \quad (1)$$

where K is the number of samples of input data $\{\mathbf{x}_k\}$ available and $\{\rho_{kj}\}$ are the elements of the input signal normalized covariance matrix ρ (see reference 1, equation (16)). Some of the problems associated with determination of the q function and its first two derivatives are discussed in reference 1.

Another problem with the realization of processor (1) is the determination of the signal normalized covariance matrix ρ . At low input SNRs, when the presence of a signal is not known and the signal has never been observed before, detailed knowledge of matrix ρ is very unlikely. The presence of signal multipaths of unknown structure, delays, and/or strengths further confounds the situation, making practical realization of processor (1) virtually impossible. Accordingly, it is desired to modify the form of the optimum processor to obviate the need for the exact signal characteristics. Also, it would be desirable to alleviate the precise determination of the derivatives of the q function and replace these functions with some simpler nonlinearities. None of these modifications can be achieved without some sacrifice of detectability performance. Therefore, any suboptimum processors must be compared with optimum processor (1) and a quantitative measure of losses ascertained, so that viable decisions can be made on the worthiness of any replacement candidates. These comparisons must be done on the basis of the receiver operating characteristics (ROCs), so that tradeoffs in false alarm probability P_f and detection probability P_d are directly quantified. Then, the differences in required input SNRs for equal detection capability (P_f, P_d) will constitute a valid basis of comparison of the various suboptimum processors, and enable a decision as to whether an acceptable alternative processor exists.

NOISE STATISTICS

Three different noise environments will be considered—Gaussian noise, sech noise, and fourth-power noise. Descriptions of all three cases follow.

GAUSSIAN NOISE

The relevant statistics of zero-mean Gaussian noise are given by

$$\begin{aligned} p(x) &= \frac{1}{\sqrt{2\pi} \sigma} \exp\left(-\frac{x^2}{2\sigma^2}\right) \text{ for all } x, \\ q(x) &= \log p(x) = -\log(\sqrt{2\pi} \sigma) - \frac{x^2}{2\sigma^2}, \\ q'(x) &= -\frac{x}{\sigma^2}, \quad q''(x) = -\frac{1}{\sigma^2}, \end{aligned} \tag{2}$$

where σ is the noise standard deviation. Device q' is linear for all input arguments; the minus factor is irrelevant in processor (1). On the other hand, nonlinearity q'' totally ignores the input data $\{\mathbf{x}_k\}$ and can be dropped from processing altogether, since additive constants do not affect the ROCs of a processor. The q functions of equation (2) are depicted in figure 1 for $\sigma = 1$. The optimum processor of equation (1) takes the form

$$\sum_{k,j=1}^K \rho_{kj} \mathbf{x}_k \mathbf{x}_j \tag{3}$$

when irrelevant scale factors and additive constants are dropped. Additional properties of Gaussian noise that are relevant to this study are given in reference 1, equations (18) through (27); in particular, compare equations (19) and (27).

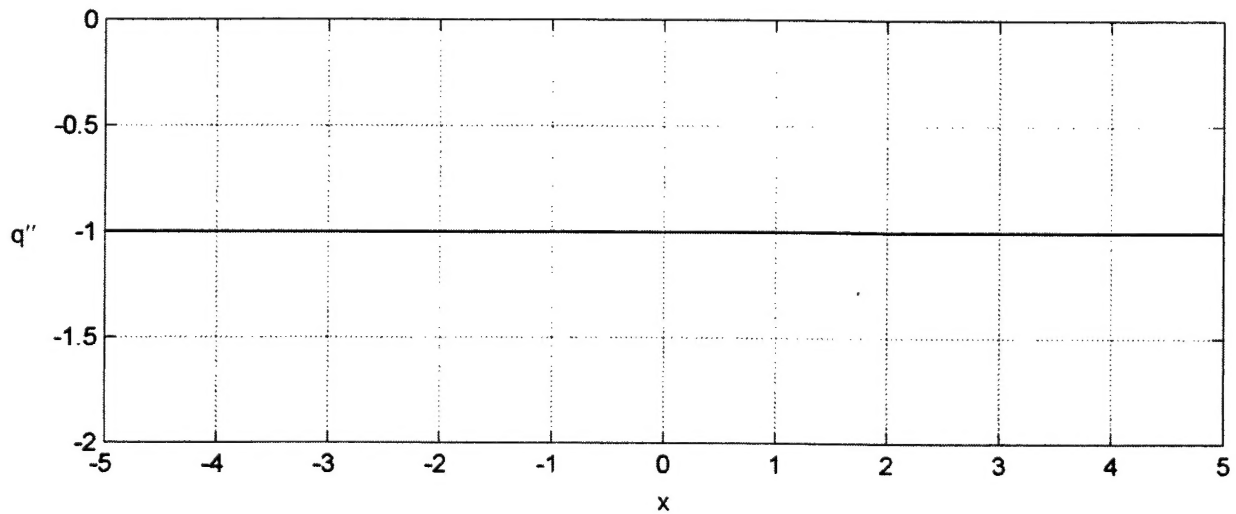
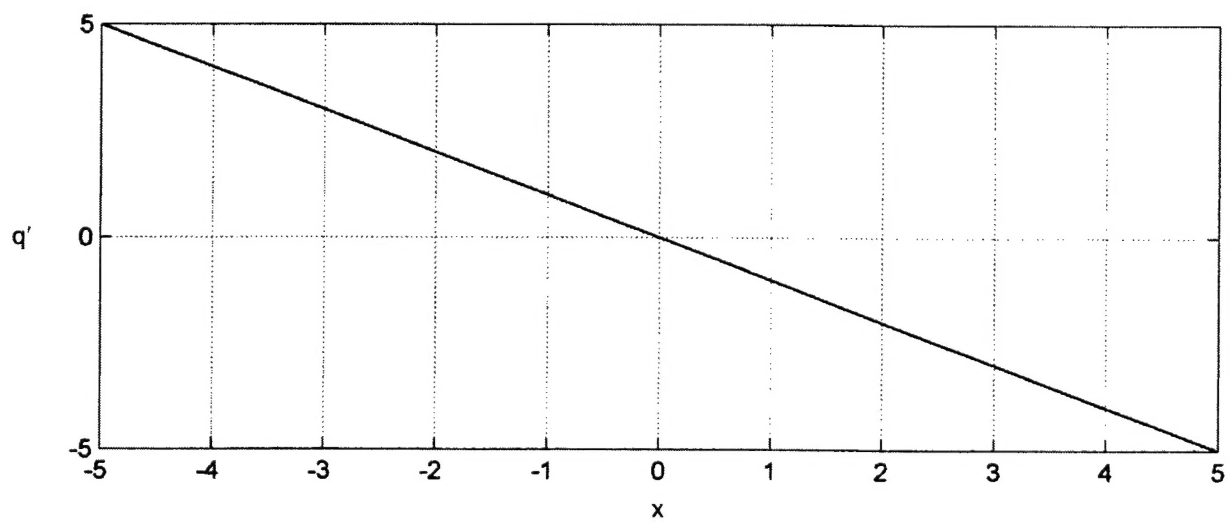
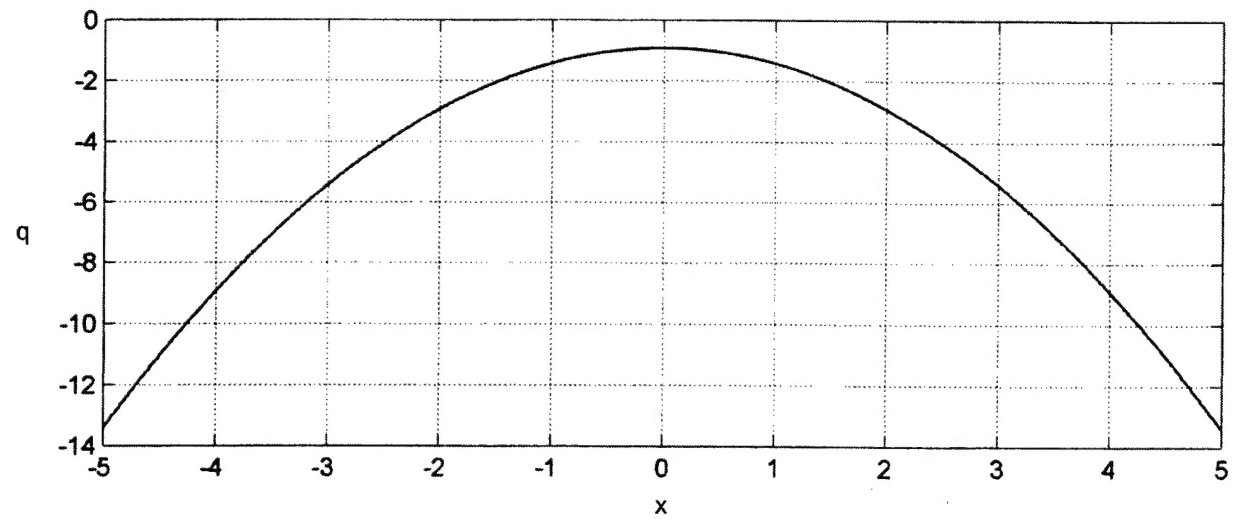


Figure 1. q Functions for Gaussian Noise, $\sigma = 1$

SECH NOISE

Sech noise is characterized by PDF

$$p(x) = \frac{1}{2\sigma} \operatorname{sech}\left(\frac{\pi}{2} \frac{x}{\sigma}\right) = \frac{1}{2\sigma} \frac{1}{\cosh\left(\frac{\pi}{2} \frac{x}{\sigma}\right)} \quad \text{for all } x, \quad (4)$$

where σ is the noise standard deviation. This PDF has exponential decay for large arguments:

$$p(x) \sim \frac{1}{\sigma} \exp\left(-\frac{\pi}{2} \frac{|x|}{\sigma}\right) \quad \text{as } x \rightarrow \pm\infty. \quad (5)$$

However, this PDF is well behaved at the origin, in distinction to exponential noise (see reference 1, equation (28) and appendix C).

The corresponding moment-generating function (MGF) is

$$\mu(\lambda) = \int dx \exp(\lambda x) p(x) = \frac{1}{\cos(\sigma \lambda)} \quad \text{for } |\lambda| < \frac{\pi}{2\sigma}, \quad (6)$$

upon use of reference 2, equation 3.511 4. Expansion of the logarithm of the MGF according to

$$\log \mu(\lambda) = \frac{1}{2}(\sigma \lambda)^2 + \frac{1}{12}(\sigma \lambda)^4 + \frac{1}{45}(\sigma \lambda)^6 + \frac{17}{2520}(\sigma \lambda)^8 + \dots \quad (7)$$

leads immediately to the nonzero cumulants

$$\chi_2 = \sigma^2, \quad \chi_4 = 2\sigma^4, \quad \chi_6 = 16\sigma^6, \quad \chi_8 = 272\sigma^8, \dots \quad (8)$$

The c -function, namely,

$$c(u, \lambda) = \int_{-\infty}^u dx \exp(\lambda x) p(x), \quad (9)$$

can be expressed only in terms of hypergeometric functions.

The cumulative distribution function (CDF) corresponding to sech PDF (4) is

$$c(x) = \int_{-\infty}^x du p(u) = \frac{2}{\pi} \operatorname{atan}\left(\exp\left(\frac{\pi}{2} \frac{x}{\sigma}\right)\right) \quad \text{for all } x. \quad (10)$$

The inverse of this CDF follows according to

$$y \equiv c(x), \quad x = \tilde{c}(y) = \sigma \frac{2}{\pi} \log \left(\tan \left(\frac{\pi}{2} y \right) \right) \quad \text{for } 0 < y < 1. \quad (11)$$

This result is needed to generate random variables (RVs) with the PDF in equation (4) from uniformly distributed RVs over (0,1).

The q functions corresponding to PDF (4) are, for all x ,

$$\begin{aligned} q(x) &= \log p(x) = -\log(2\sigma) - \log \left(\cosh \left(\frac{\pi}{2} \frac{x}{\sigma} \right) \right), \\ q'(x) &= -\frac{1}{\sigma} \frac{\pi}{2} \tanh \left(\frac{\pi}{2} \frac{x}{\sigma} \right), \\ q''(x) &= -\frac{1}{\sigma^2} \frac{\pi^2}{4} \operatorname{sech}^2 \left(\frac{\pi}{2} \frac{x}{\sigma} \right) = q'(x)^2 - \frac{1}{\sigma^2} \frac{\pi^2}{4}. \end{aligned} \quad (12)$$

These functions are depicted in figure 2 for $\sigma = 1$. The $q'(x)$ function has slope $-\frac{1}{\sigma^2} \frac{\pi^2}{4}$ at the origin and rapidly saturates at values $\pm \frac{1}{\sigma} \frac{\pi}{2}$ as $|x|$ exceeds σ ; thus, this nonlinearity behaves as a soft limiter. The $q''(x)$ function has a negative bump at the origin of magnitude $\frac{1}{\sigma^2} \frac{\pi^2}{4}$ and decays rapidly to zero for large x ; in fact, its major contribution takes place only for $|x|$ within σ of the origin. There are no anomalies in the behavior of function $q''(x)$ at the origin, as there are for the exponential PDF $2^{-1/2}/\sigma \exp(-2^{1/2} |x|/\sigma)$.

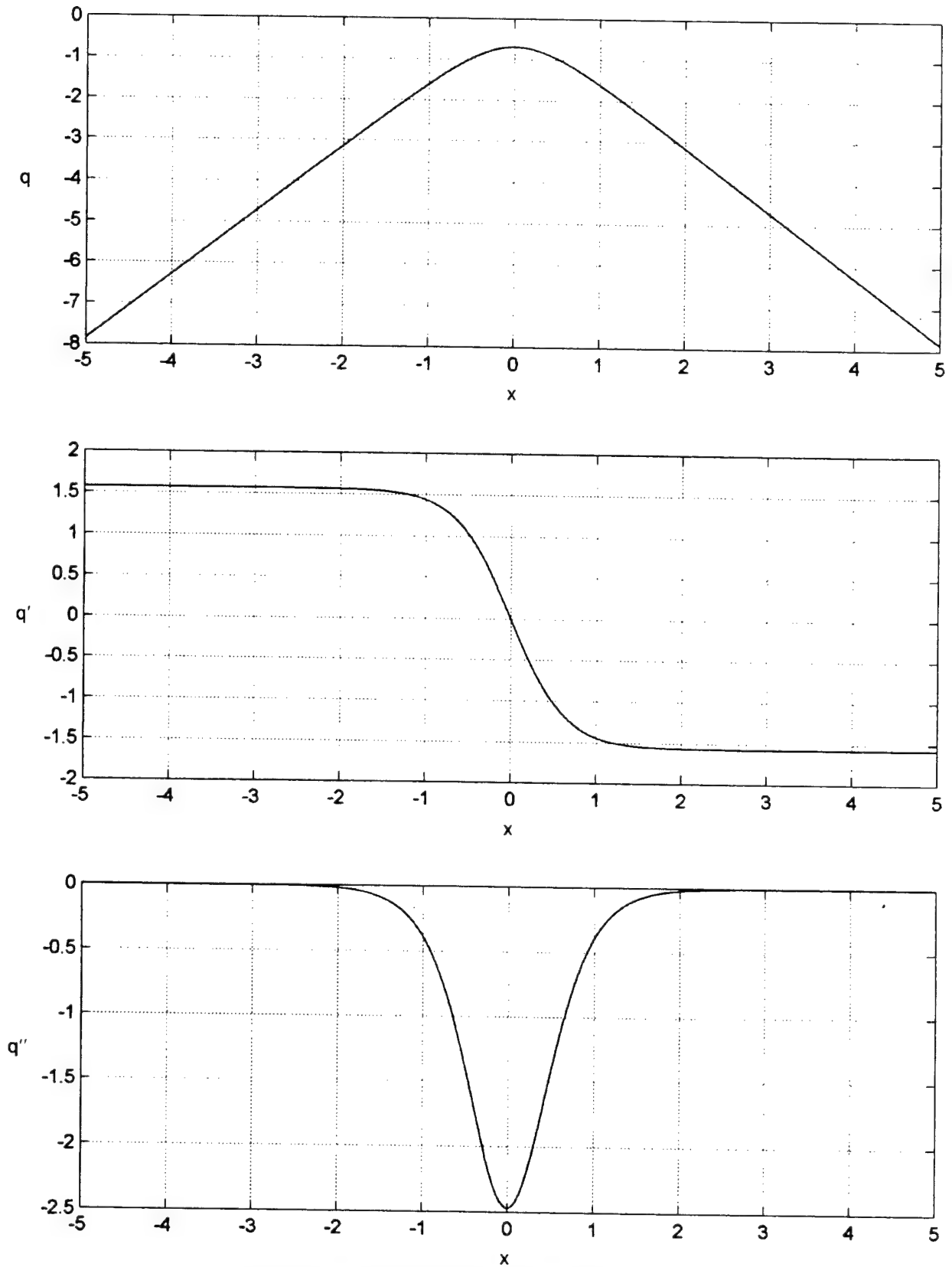


Figure 2. q Functions for Sech Noise, $\sigma = 1$

The optimum processor for noise PDF (4) takes the form

$$\begin{aligned}
 \mathbf{L} &= \sum_{k=1}^K q''(\mathbf{x}_k) + \sum_{k,j=1}^K \rho_{kj} q'(\mathbf{x}_k) q'(\mathbf{x}_j) \\
 &= \frac{1}{\sigma^2} \frac{\pi^2}{4} \left(\sum_{k,j=1}^K \rho_{kj} \tanh(\mathbf{a}_k) \tanh(\mathbf{a}_j) - \sum_{k=1}^K \text{sech}^2(\mathbf{a}_k) \right) \\
 &= \frac{1}{\sigma^2} \frac{\pi^2}{4} \left(\sum_{k,j=1}^K \rho_{kj} \tanh(\mathbf{a}_k) \tanh(\mathbf{a}_j) + \sum_{k=1}^K \tanh^2(\mathbf{a}_k) - K \right), \tag{13}
 \end{aligned}$$

where RV

$$\mathbf{a}_k = \frac{\pi}{2} \frac{\mathbf{x}_k}{\sigma} \quad \text{for } k = 1 : K. \tag{14}$$

The leading scale factor in the second and third lines of equation (13) can be dropped without affecting the performance of the optimum processor; however, the scale factor relating \mathbf{a}_k to \mathbf{x}_k must be retained and utilized. Therefore, the noise standard deviation σ must be known.

PDF of Sum of Independent Sech RVs

The characteristic function (CF) of a sech RV is available from the MGF in equation (6) as

$$\mu(i\xi) = \int dx \exp(i\xi x) p(x) = \frac{1}{\cos(i\sigma\xi)} = \frac{1}{\cosh(\sigma\xi)} \quad \text{for all real } \xi, \tag{15}$$

which has the identical form as the PDF in equation (4). Therefore, the CF of a sum u of n independent sech RVs with the same standard deviation is

$$\mu_n(i\xi) = \frac{1}{\cosh^n(\sigma\xi)}. \tag{16}$$

Thus, the PDF of the sum u is given by the Fourier transform

$$\begin{aligned}
 p_n(u) &= \frac{1}{2\pi} \int_{-\infty}^{\infty} d\xi \frac{\exp(-iu\xi)}{\cosh^n(\sigma\xi)} = \frac{1}{\pi} \int_0^{\infty} d\xi \frac{\cos(u\xi)}{\cosh^n(\sigma\xi)} = \frac{2^{n-2}}{\pi\sigma} B\left(\frac{n}{2} + \frac{iu}{2\sigma}, \frac{n}{2} - \frac{iu}{2\sigma}\right) \\
 &= \frac{2^{n-2}}{(n-1)! \pi\sigma} \Gamma\left(\frac{n}{2} + \frac{iu}{2\sigma}\right) \Gamma\left(\frac{n}{2} - \frac{iu}{2\sigma}\right) = \frac{2^{n-2}}{(n-1)! \pi\sigma} \left| \Gamma\left(\frac{n}{2} + \frac{iu}{2\sigma}\right) \right|^2, \tag{17}
 \end{aligned}$$

upon use of reference 2, equations 3.512 1 and 8.380 1, and reference 3, equation 6.1.23.

Closed forms can be developed for this PDF for any n . By using reference 3, equations 6.1.15, 6.1.30, and 6.1.31, the following examples were developed:

$$\begin{aligned}
p_1(u) &= \frac{1}{2\sigma} \frac{1}{\cosh(U)}, \quad U \equiv \frac{\pi u}{2\sigma} \quad (\text{in agreement with equation (3)}), \\
p_2(u) &= \frac{1}{\pi\sigma} \frac{U}{\sinh(U)}, \\
p_3(u) &= \frac{1}{4\sigma} \left(1 + \frac{u^2}{\sigma^2}\right) \frac{1}{\cosh(U)}, \\
p_4(u) &= \frac{1}{6\pi\sigma} \left(4 + \frac{u^2}{\sigma^2}\right) \frac{U}{\sinh(U)}, \\
p_5(u) &= \frac{1}{48\sigma} \left(9 + \frac{u^2}{\sigma^2}\right) \left(1 + \frac{u^2}{\sigma^2}\right) \frac{1}{\cosh(U)}, \\
p_6(u) &= \frac{1}{120\pi\sigma} \left(16 + \frac{u^2}{\sigma^2}\right) \left(4 + \frac{u^2}{\sigma^2}\right) \frac{U}{\sinh(U)}.
\end{aligned} \tag{18}$$

In fact, a simple recursive formula for the n th PDF follows readily from equation (17):

$$p_n(u) = p_{n-2}(u) \frac{(n-2)^2 + u^2/\sigma^2}{(n-1)(n-2)} \quad \text{for } n \geq 3. \tag{19}$$

Starting values are available from equation (18).

FOURTH-POWER NOISE

The PDF for this type of noise is given by

$$p(x) = \frac{1}{\sigma} \frac{3/(\sqrt{2}\pi)}{\left(1 + \frac{2x^2}{\sigma^2}\right)\left(1 + \frac{x^2}{2\sigma^2}\right)} = \frac{1}{\sigma\sqrt{2}\pi} \left(\frac{4}{1 + \frac{2x^2}{\sigma^2}} - \frac{1}{1 + \frac{x^2}{2\sigma^2}} \right) \quad \text{for all } x, \tag{20}$$

where σ is the noise standard deviation. For large arguments, this PDF decays only as $1/x^4$, which constitutes a very heavy-tailed (HT) distribution. The corresponding CF is

$$\mu(i\xi) = 2 \exp(-|\xi|\sigma/\sqrt{2}) - \exp(-|\xi|\sigma\sqrt{2}) \quad \text{for all real } \xi. \tag{21}$$

The $c(u, \lambda)$ function of equation (9) involves four exponential integrals.

The CDF for fourth-power PDF (20) is

$$c(x) = \frac{1}{2} + \frac{1}{\pi} \left[2 \operatorname{atan} \left(\frac{\sqrt{2} x}{\sigma} \right) - \operatorname{atan} \left(\frac{x}{\sqrt{2} \sigma} \right) \right] = \frac{2}{\pi} \operatorname{atan} \left(\exp \left(3 \operatorname{asinh} \left(\frac{x}{\sqrt{2} \sigma} \right) \right) \right). \quad (22)$$

The inverse to this relation, $y = c(x)$, is given by

$$x = \tilde{c}(y) = \sigma \sqrt{2} \sinh \left(\frac{1}{3} \log \left(\tan \left(\frac{\pi}{2} y \right) \right) \right) \quad \text{for } 0 < y < 1. \quad (23)$$

The derivation of the last two relations is given in appendix A. Result (23) allows for rapid generation of RVs with fourth-power PDF (19) directly from uniformly distributed RVs over $(0,1)$.

The q functions for fourth-power PDF (20) are

$$\begin{aligned} q(x) &= \log p(x) = \log \left(\frac{3}{\sqrt{2} \pi \sigma} \right) - \log \left(1 + \frac{2x^2}{\sigma^2} \right) - \log \left(1 + \frac{x^2}{2\sigma^2} \right), \\ q'(x) &= -\frac{4x}{\sigma^2 + 2x^2} - \frac{2x}{2\sigma^2 + x^2}, \\ q''(x) &= -4 \frac{\sigma^2 - 2x^2}{(\sigma^2 + 2x^2)^2} - 2 \frac{2\sigma^2 - x^2}{(2\sigma^2 + x^2)^2} \quad \text{for all } x. \end{aligned} \quad (24)$$

These functions are depicted in figure 3 for $\sigma = 1$. Function q' is linear for small arguments, but then saturates and returns slowly to zero as $-4/x$ for large x . The second derivative q'' has a large negative bump near the origin and returns to zero as $4/x^2$ for large x . The optimum processor is available upon reference to equation (1).

Plots of the three types of noise processes are given in figure 4 for a standard deviation of $\sigma = 1$. Whereas the Gaussian sample data are limited to a range of ± 3 , the sech noise sample reaches values of ± 5 , and the fourth-power noise sample attains values near ± 10 . Also, the burst-like character of the fourth-power noise is very obvious, occasionally reaching values many times that of its standard deviation. It is these bursts that cause serious degradation of performance of processors designed to operate in a Gaussian noise background.

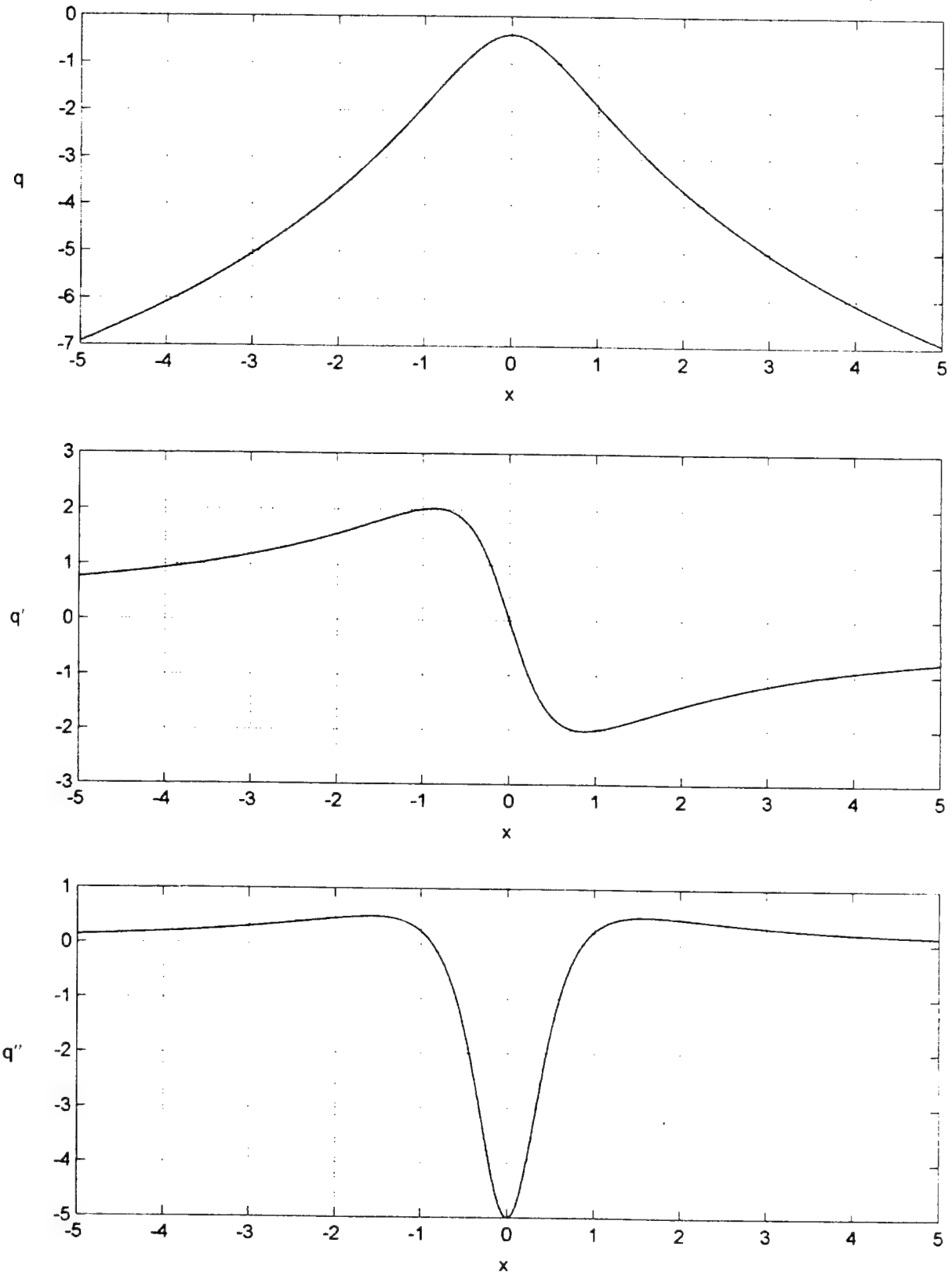


Figure 3. q Functions for Fourth-Power Noise, $\sigma = 1$

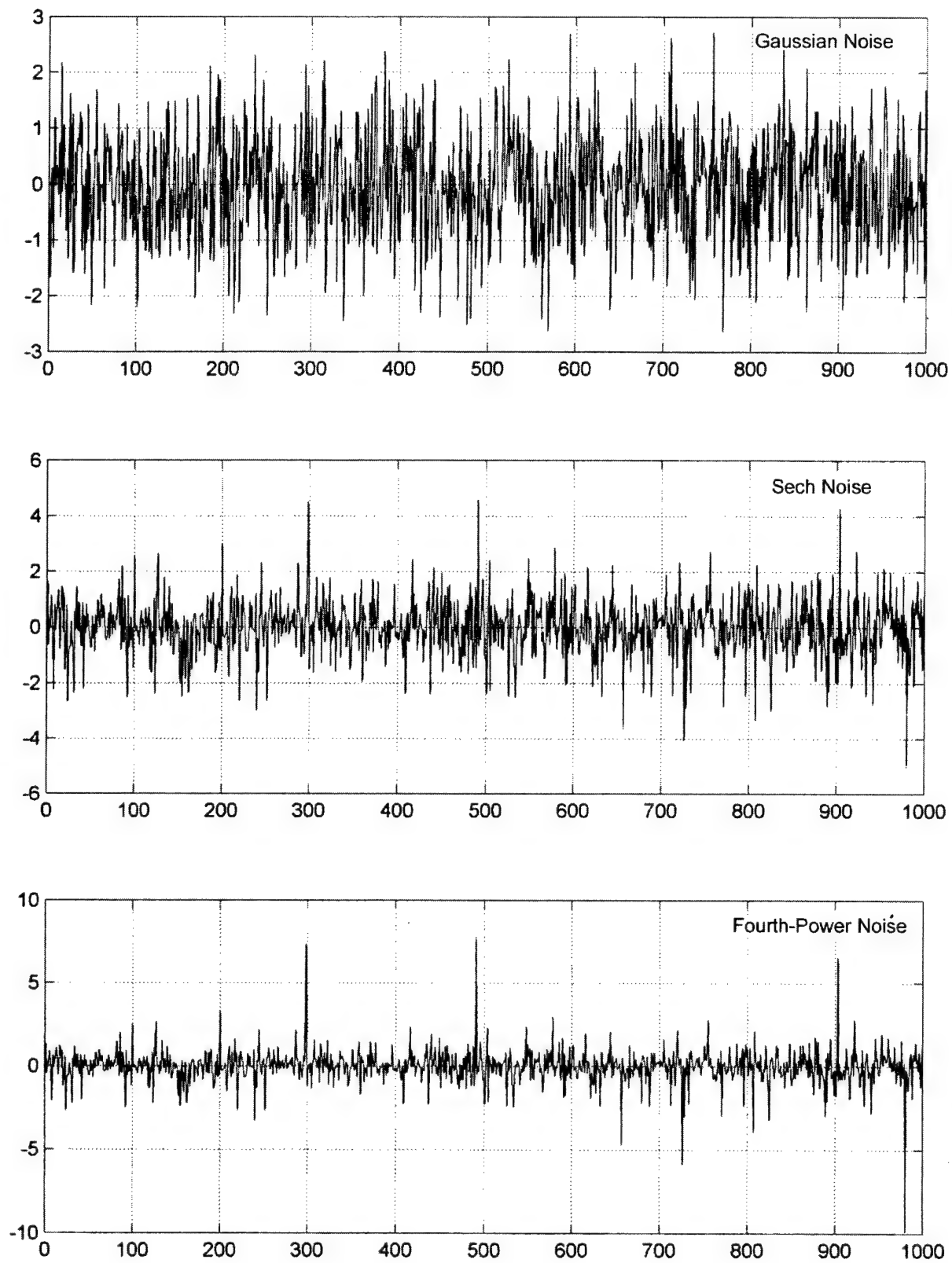


Figure 4. Sample Data Sequences of 1000 Independent Variables

q FUNCTIONS FOR NONLINEARLY TRANSFORMED RANDOM VARIABLES

The three noise processes discussed above were generated directly from uniformly distributed RVs over (0,1). An alternative method of generating RVs is by means of nonlinear transformations of RVs with already established statistics (other than uniform). Here, RV y will be generated from RV x according to monotonically increasing transformation f : $y = f(x)$. Random variable x has PDF $p_x(x)$ and corresponding (zeroth-order) q function

$$q_x(x) = \log p_x(x). \quad (25)$$

The first nonlinear transformation of interest is cubic, resulting in RV

$$y = x + ax^3, \quad a > 0 \quad (\text{for monotonicity}). \quad (26)$$

Let

$$y = f(x) = x + ax^3, \quad f'(x) = 1 + 3ax^2, \quad x = \tilde{f}(y) \equiv F, \quad (27)$$

where \tilde{f} denotes the inverse function to f . This inverse function is given by

$$F = \tilde{f}(y) = t(y) - \frac{1}{3at(y)}, \quad t(y) = \left(\frac{y}{2a} + \sqrt{\left(\frac{y}{2a} \right)^2 + \frac{1}{27a^3}} \right)^{1/3} \quad (28)$$

(see reference 1, equations (42) through (46)). Then, upon use of equation (27),

$$F' = \tilde{f}'(y) = \frac{1}{f'(\tilde{f}(y))} = \frac{1}{f'(F)} = \frac{1}{1 + 3aF^2}. \quad (29)$$

This result affords a simple technique of finding higher-order derivatives of inverse function F . The PDF of RV y is given by

$$p_y(y) = \frac{p_x(\tilde{f}(y))}{f'(\tilde{f}(y))} = \frac{p_x(F)}{f'(F)} = \frac{p_x(F)}{1 + 3aF^2}. \quad (30)$$

As an example of an application, let RV x be zero-mean Gaussian with standard deviation σ . Then, the PDF of $y = x + ax^3$ is

$$p_y(y) = \frac{1}{\sqrt{2\pi}\sigma} \frac{\exp(-F^2/(2\sigma^2))}{1 + 3aF^2}. \quad (31)$$

The first three q functions follow immediately upon use of equations (29) and (30) as

$$\begin{aligned}
q_y(y) &= \log p_y(y) = -\log(\sqrt{2\pi}\sigma) - \frac{F^2}{2\sigma^2} - \log(1 + 3aF^2), \\
q'_y(y) &= -\frac{1}{\sigma^2} \frac{F}{1 + 3aF^2} - 6a \frac{F}{(1 + 3aF^2)^2}, \\
q''_y(y) &= -\frac{1}{\sigma^2} \frac{1 - 3aF^2}{(1 + 3aF^2)^3} - 6a \frac{1 - 9aF^2}{(1 + 3aF^2)^4}.
\end{aligned} \tag{32}$$

These equations quickly confirm the numerical results in reference 1, figure 3, which were obtained by a much more laborious technique involving symbolic differentiation. The function F is given by equation (28) above. These results allow for realization of the optimum processor in equation (1).

Plots of the q functions in equation (32) are displayed in figures 5, 6, 7, and 8 for scale factor a equal to 0.1, 0.2, 0.3, and 0.4, respectively ($a = 0$ corresponds to a Gaussian RV). The four q functions in the uppermost subplots gradually develop a more pronounced flare for large arguments y , as a increases. Also, the q'' functions develop a progressively larger negative bump near the origin. The gradual narrowing of the various functions in y in the figures is due to the standard deviation of RV y increasing as a increases; thus, the standard deviations of y for the scale factors detailed above are 1.32, 1.67, 2.04, and 2.41, respectively. That is, abscissa value $y = 1$ in the figures does not correspond to unit standard deviation, as it did in the earlier figures.

As $y \rightarrow +\infty$, the asymptotic behaviors of the functions above are according to

$$\begin{aligned}
t(y) &\sim (y/a)^{1/3}, \quad F \sim (y/a)^{1/3}, \quad q_y(y) \sim -\frac{(y/a)^{2/3}}{2\sigma^2} = \frac{-1}{2a^{2/3}\sigma^2} y^{2/3}, \\
q'_y(y) &\sim \frac{-1}{3a^{2/3}\sigma^2} \frac{1}{y^{1/3}}, \quad q''_y(y) \sim \frac{1}{9a^{2/3}\sigma^2} \frac{1}{y^{4/3}}, \\
p_y(y) &= \exp(q_y(y)) \sim \exp\left(-\frac{1}{2\sigma^2} \left(\frac{y}{a}\right)^{2/3}\right).
\end{aligned} \tag{33}$$

Thus, both derivatives of the $q_y(y)$ function decay to zero for large arguments, albeit at very slow rates, especially for the first derivative. The decay of the PDF of y is slower than exponential. All the results above apply only to a Gaussian RV x and cubic nonlinear transformation (26).

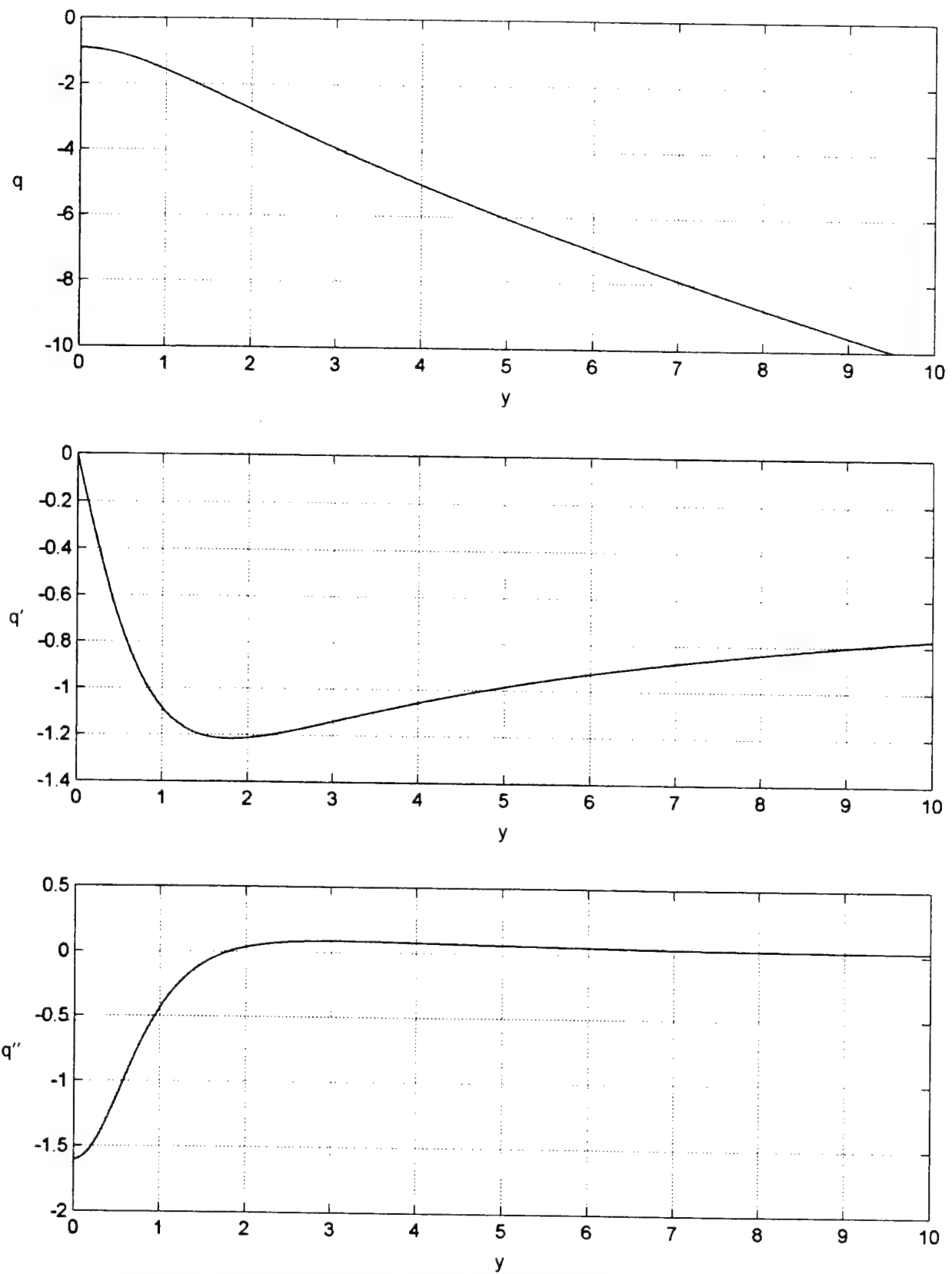


Figure 5. q Functions for Cubic Transformation, $a = 0.1, \sigma_y = 1.32$

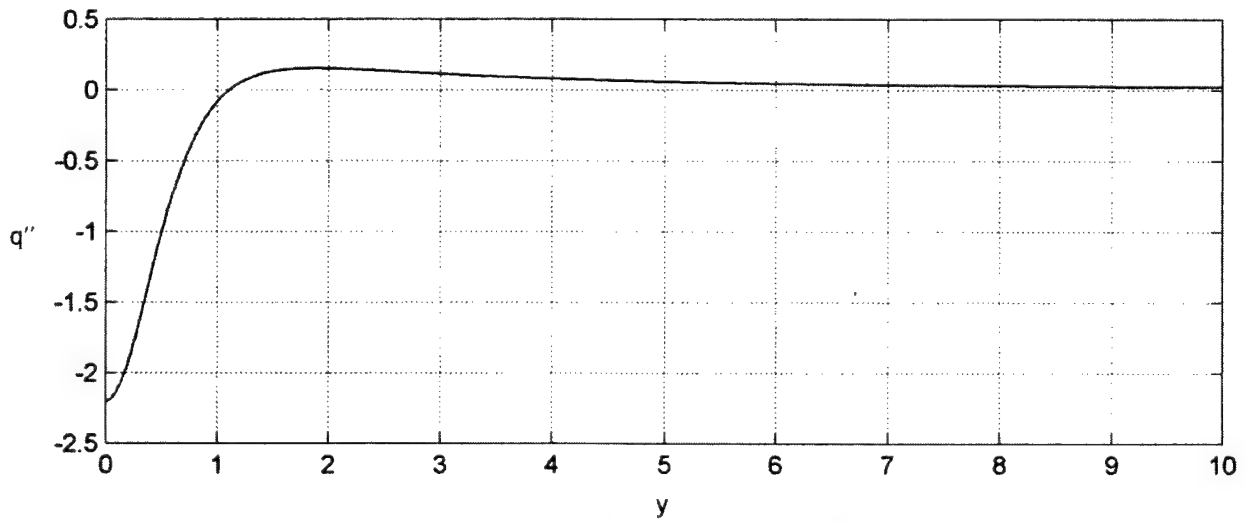
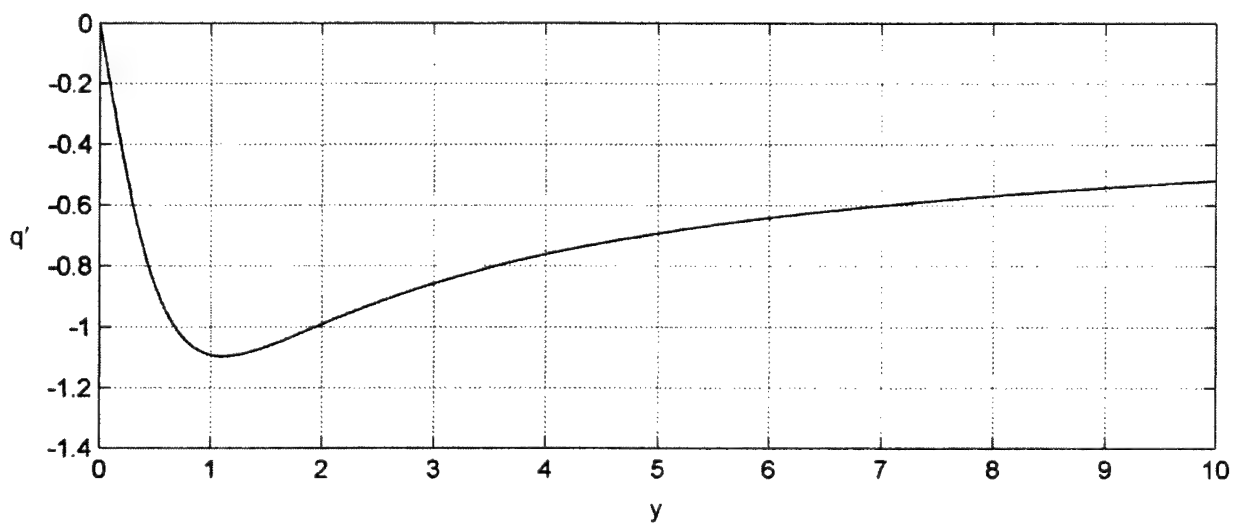
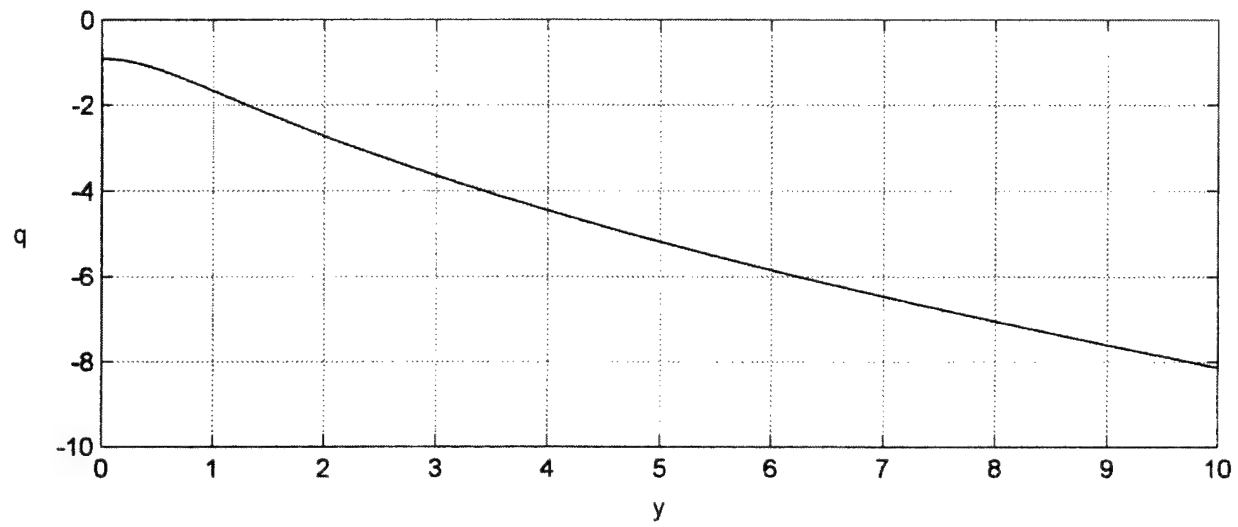


Figure 6. q Functions for Cubic Transformation, $a = 0.2, \sigma_y = 1.67$

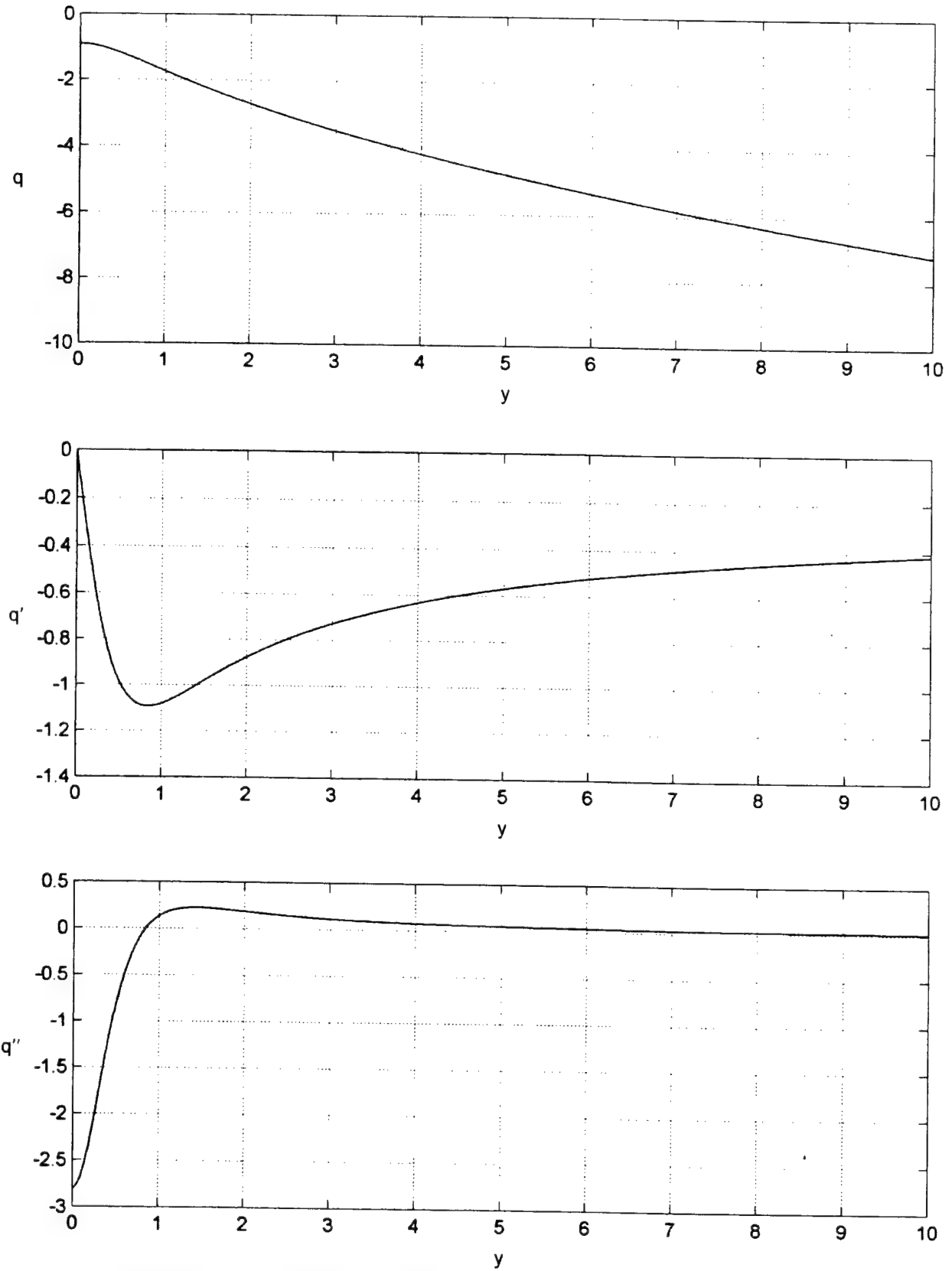


Figure 7. q Functions for Cubic Transformation, $a = 0.3, \sigma_y = 2.04$

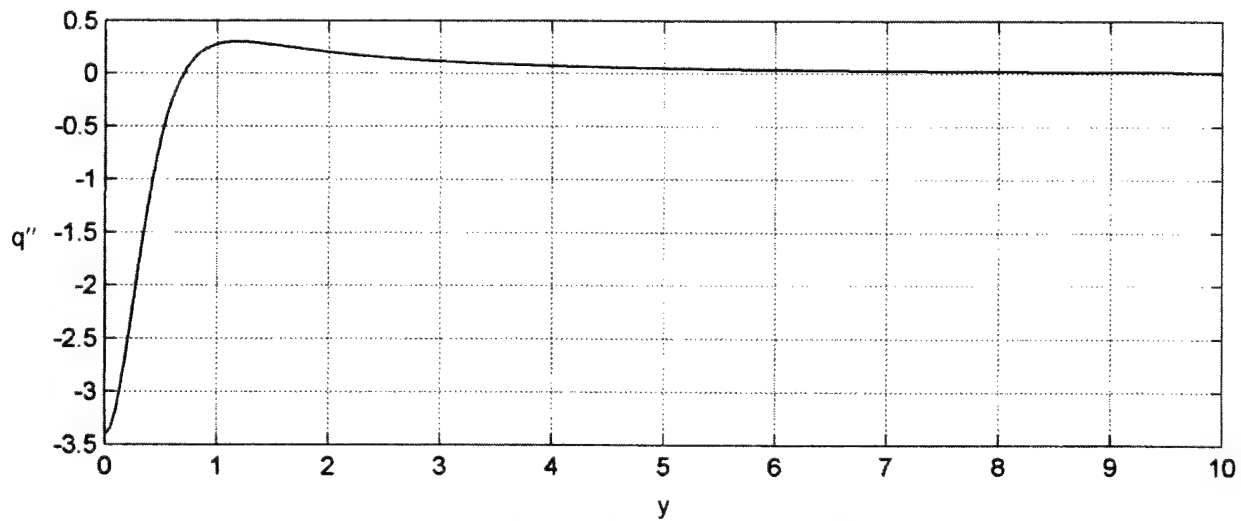
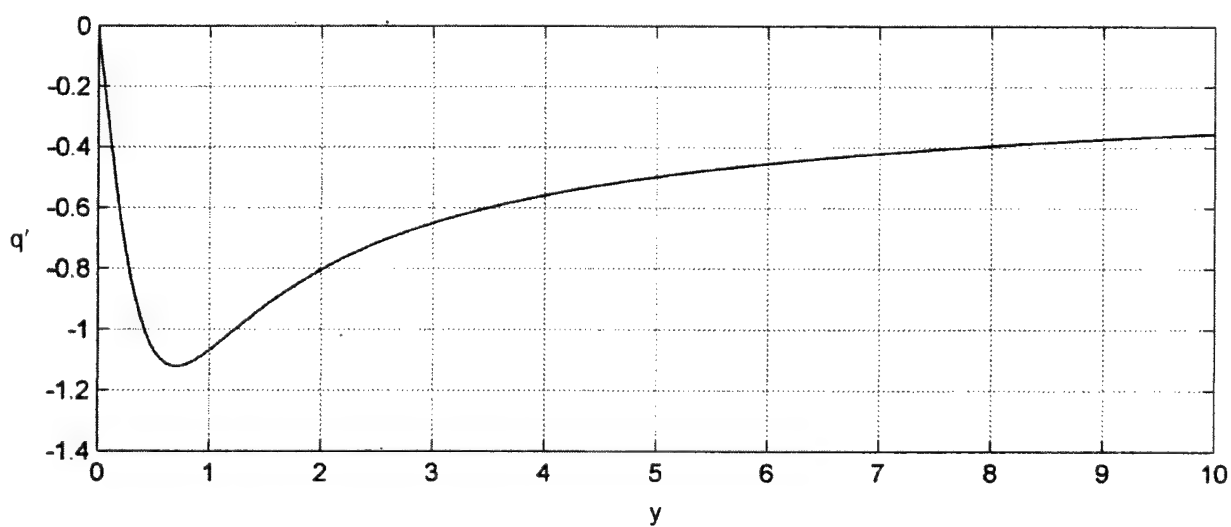
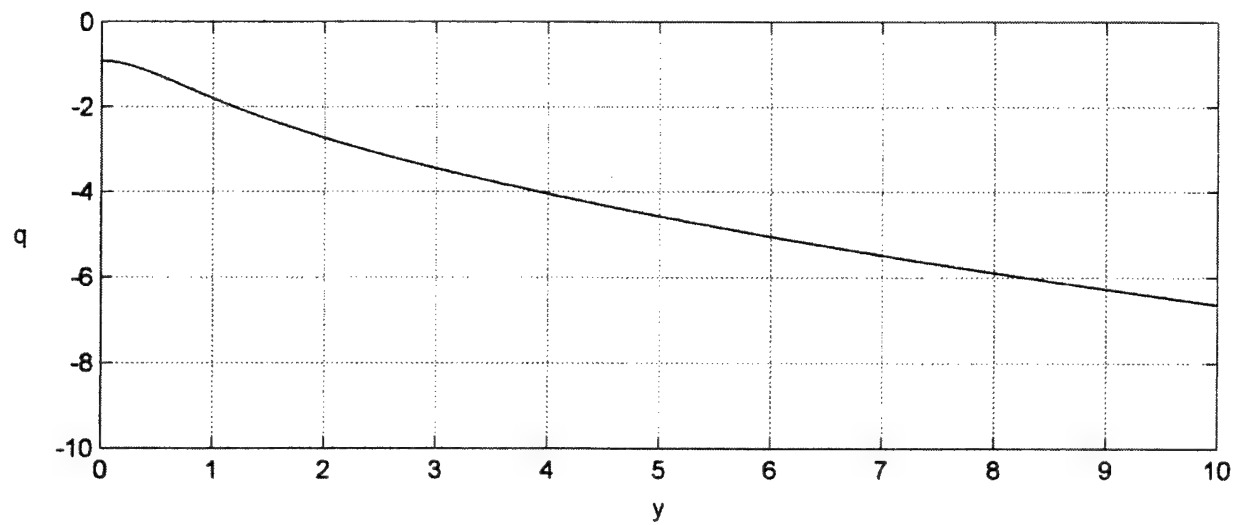


Figure 8. q Functions for Cubic Transformation, $a = 0.4, \sigma_y = 2.41$

More generally, for an arbitrary monotonically increasing nonlinear transformation f and input PDF p_x , the relevant transformations are defined according to

$$y = f(x), \quad x = g(y), \quad (34)$$

where g is the inverse function to f . It is presumed that function f and its derivatives can be readily evaluated. The CDF of RV $y = f(x)$ is given by

$$c_y(y) = \Pr(y < y) = \Pr(f(x) < y) = \Pr(x < g(y)) = c_x(g(y)). \quad (35)$$

The corresponding PDF of y is

$$p_y(y) = c'_y(y) = c'_x(g(y)) g'(y) = p_x(g(y)) g'(y). \quad (36)$$

But, from equation (34),

$$y = f(g(y)), \quad 1 = f'(g(y)) g'(y), \quad g'(y) = \frac{1}{f'(g(y))}. \quad (37)$$

This relation avoids the need to evaluate the derivative of the inverse function g . Substitution of equation (37) in equation (36) yields

$$p_y(y) = \frac{p_x(g(y))}{f'(g(y))}. \quad (38)$$

The zeroth-order q function for RV y is

$$q_y(y) = \log p_y(y) = \log p_x(g(y)) - \log f'(g(y)) = q_x(g(y)) - \log f'(g(y)). \quad (39)$$

The first derivative follows as

$$q'_y(y) = \frac{q'_x(g(y))}{f'(g(y))} - \frac{f''(g(y))}{f'(g(y))^2}, \quad (40)$$

where equation (37) has been used. The second derivative follows in a similar manner as

$$q''_y(y) = \frac{q''_x(g(y)) f'(g(y)) - q'_x(g(y)) f''(g(y))}{f'(g(y))^3} - \frac{f'''(g(y)) f'(g(y)) - 2 f''(g(y))^2}{f'(g(y))^4}. \quad (41)$$

The functions needed are the q functions for RV x , the transformation f and its first three derivatives, and the inverse function g .

If inverse function g cannot be determined analytically, the following numerical approach will yield sample values of the desired q functions of RV y . Select a set of fine spacings in x ,

namely, $\{x_n\}$ for $n = 1 : N$, where N is large enough to cover the range of interest. Then, from transformation (34), evaluate and store the values

$$y_n = f(x_n) \text{ for } n = 1 : N; \text{ equivalently, } x_n = g(y_n). \quad (42)$$

Now, equations (39) through (41) immediately yield, for $n = 1 : N$,

$$\begin{aligned} q_y(y_n) &= q_x(x_n) - \log f'(x_n), \\ q'_y(y_n) &= \frac{q'_x(x_n)}{f'(x_n)} - \frac{f''(x_n)}{f'(x_n)^2}, \\ q''_y(y_n) &= \frac{q''_x(x_n) f'(x_n) - q'_x(x_n) f''(x_n)}{f'(x_n)^3} - \frac{f'''(x_n) f'(x_n) - 2 f''(x_n)^2}{f'(x_n)^4}. \end{aligned} \quad (43)$$

All of the quantities needed here are readily available from the tabulation in equation (42).

PERFORMANCE OF OPTIMUM PROCESSORS IN NON-GAUSSIAN NOISE

The background noise will be taken to be one of the three types introduced in the previous section; namely, Gaussian noise, sech noise, or fourth-power noise. The signal, when present, will be the multipath model given in reference 1, page 9. Namely, signal sample

$$\mathbf{s}_k = \mathbf{d}_k + \alpha \mathbf{d}_{k-m}, \quad m > 0, \quad (44)$$

for $k = 1 : K$, where zero-mean sequence $\{\mathbf{d}_k\}$ consists of uncorrelated samples. In all the following numerical results, the number of independent noise data samples is $K = 1000$, the signal delay is $m = 10$, and the relative attenuation factor is $\alpha = -1$, corresponding to a perfectly reflecting surface-bounce path. The ROCs have been generated by using one million trials for each processor and signal-noise combination of interest. The input SNR is the ratio of the total power in signal sample (44) to the noise power per sample.

The initial ROCs in figure 9 pertain to the usual reference case, namely, the optimum processor for Gaussian signal in Gaussian noise (see equation (3) and reference 1, equation (35)). Equation (3) will be referred to as Processor G. Signal parameters α and m are presumed known to the receiver processor. Three operating points (OPs) are of particular interest: low-quality OP $P_f = 1e-3$, $P_d = 0.5$; medium-quality OP $P_f = 1e-4$, $P_d = 0.9$; and high-quality OP $P_f = 1e-5$, $P_d = 0.99$. The required input SNRs to realize these three OPs are observed to be -9.2 dB, -6.8 dB, and -5.3 dB, respectively. These numerical results are consistent with the original derivation in reference 1, which was for low input SNRs.

The ROCs in figure 10 differ only in that the background is changed to sech noise, while the processor is *kept* as equation (3), with all signal parameters known, namely, Processor G. This is *not* the optimum processor for a sech noise background. The required SNRs at the low-, medium-, and high-quality OPs are -7.85 dB, -5.6 dB, and -4.1 dB, respectively. These values are not significantly different from those in figure 9, being approximately 1.2 dB worse.

However, when the background is changed to fourth-power noise and the processor is still unchanged from that above, the ROCs indicate grossly degraded performance, as shown in figure 11. The required input SNR to realize the low-quality OP is approximately $+6$ dB, a whopping 15-dB degradation relative to the Gaussian background case. This example demonstrates the dangers in trying to use the processor designed for Gaussian interference, namely, Processor G, in the presence of HT noise, even when the signal parameters are exactly known. The losses for this suboptimum processor at the medium- and high-quality OPs are still worse and were not estimated.

To determine bases of performance in non-Gaussian noise backgrounds, the optimum processors for those environments must be investigated quantitatively. The optimum processor for a sech noise background was presented in equation (13) and is denoted as Processor S. The optimum processor for a fourth-power noise background is available upon combination of equations (1) and (24) and is denoted as Processor F. These optimum processors require and utilize knowledge of the signal characteristics and parameters.

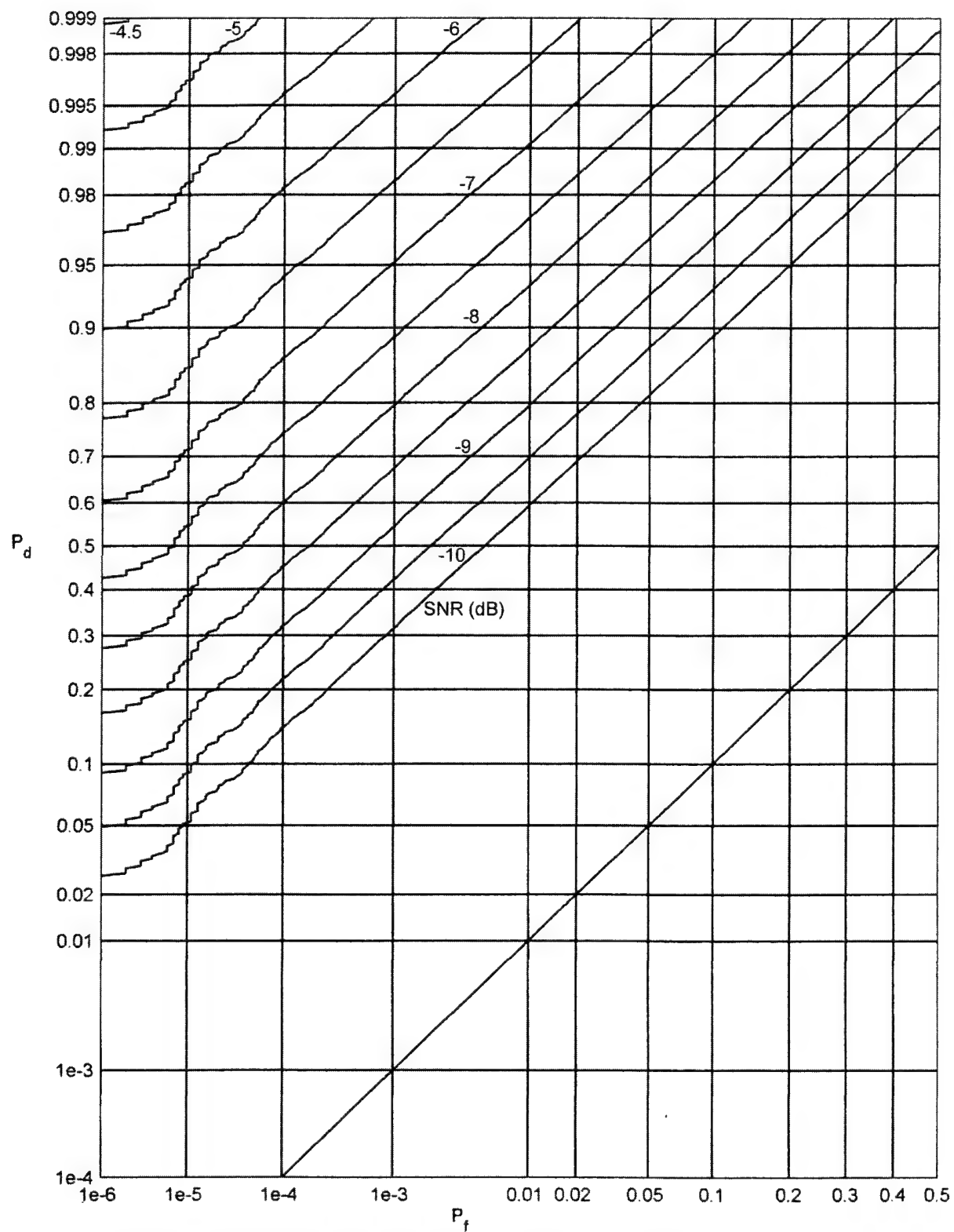


Figure 9. ROCs for Gaussian Signal in Gaussian Noise, Processor G

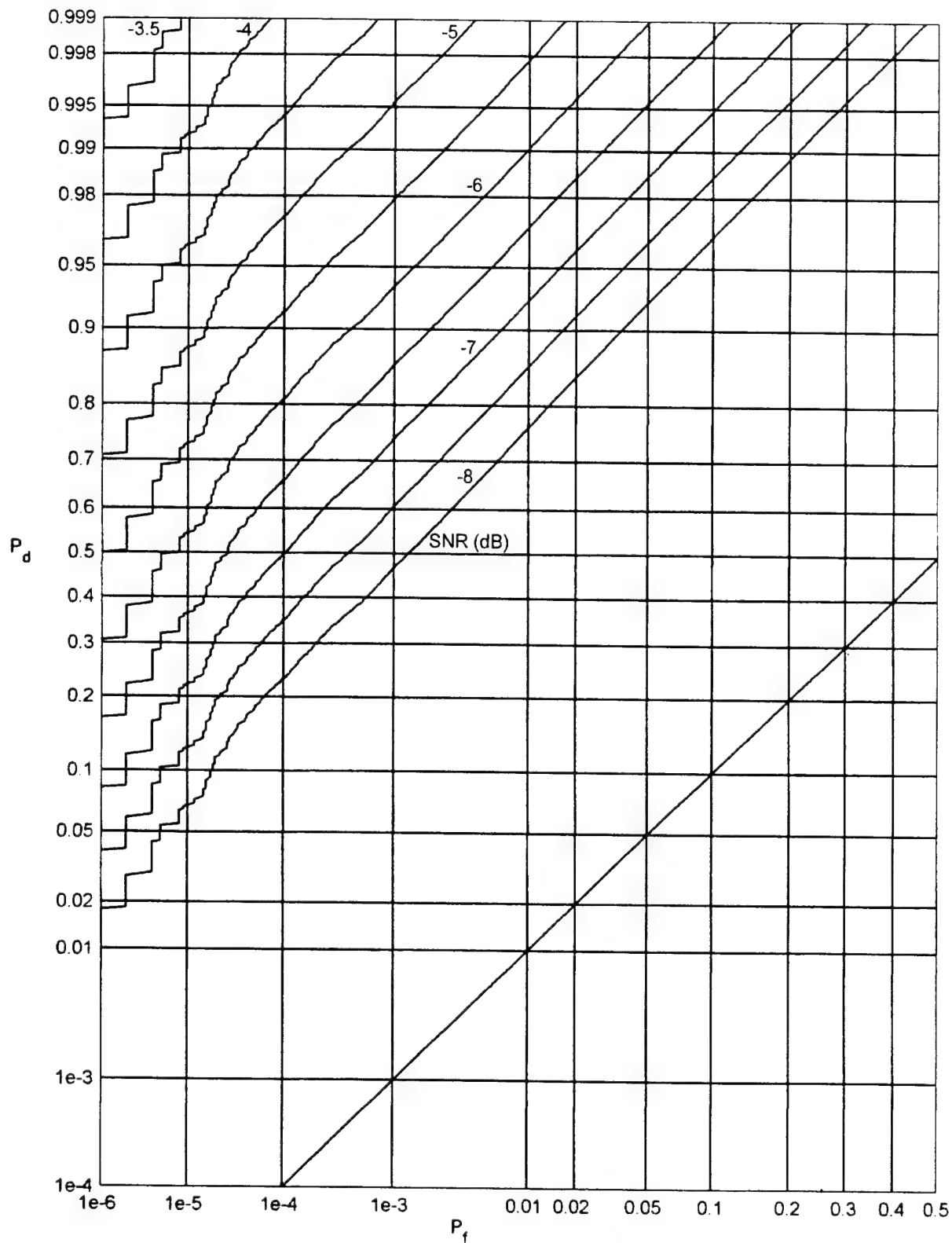


Figure 10. ROCs for Gaussian Signal in Sech Noise, Processor G

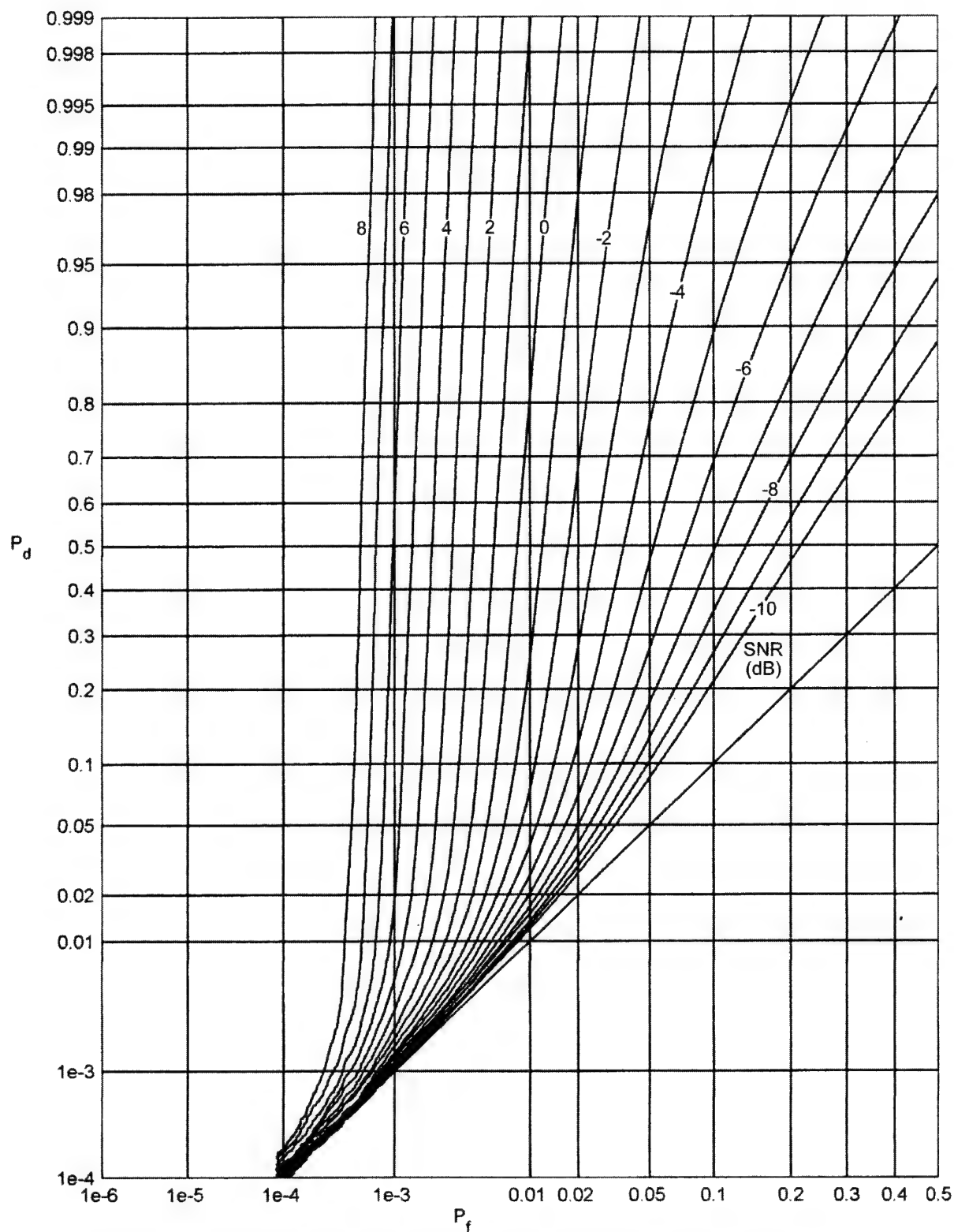


Figure 11. ROCs for Gaussian Signal in Fourth-Power Noise, Processor G

To determine the fundamental capability of detection in sech noise, and to ascertain the dependence on the particular *signal* type, the ROCs in figures 12 through 14 were generated. All three cases utilize Processor S, while the signal is alternatively Gaussian, sech, and fourth-power, respectively. The required input SNRs are rather similar for the Gaussian and sech signal cases, while those for the fourth-power signal are about 1.1 to 1.7 dB larger. Thus, the optimum detectability does vary slightly with the signal type, with the Gaussian signal being most detectable and the fourth-power signal being the least detectable. The HT character of the fourth-power signal does not help detectability for low input SNRs.

The corresponding results for optimum detection in fourth-power noise, that is, for processor F, are presented in figures 15 through 17. The three sets of ROCs correspond to Gaussian, sech, and fourth-power signals, respectively. Again, the required input SNRs for the Gaussian and sech signal cases are rather similar, while those for the fourth-power signal are about 1.2 to 2.2 dB larger, depending on the exact operating point of interest. Alternative operating points can easily be investigated from the ROCs presented in figures 9 through 17.

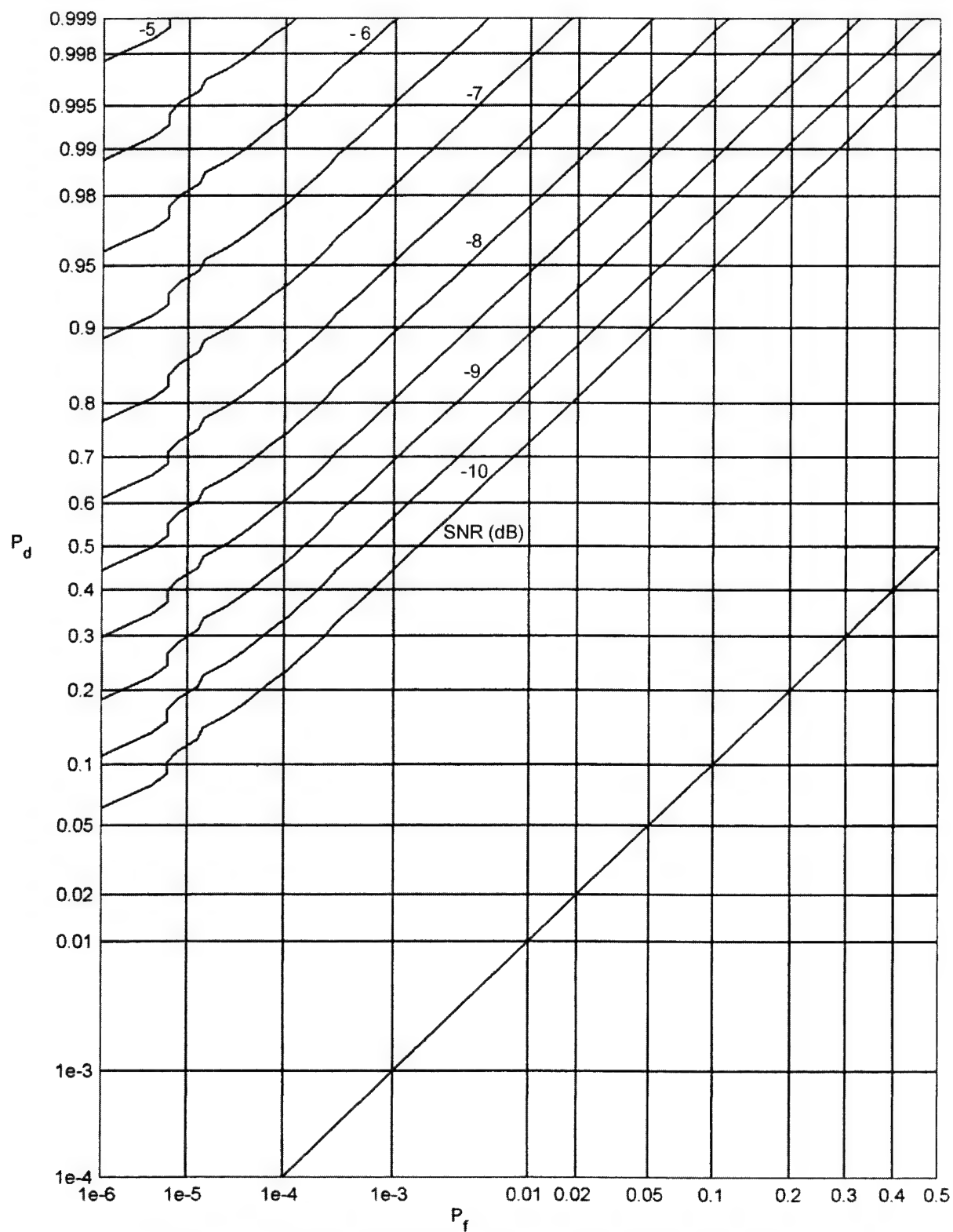


Figure 12. ROCs for Gaussian Signal in Sech Noise, Processor S

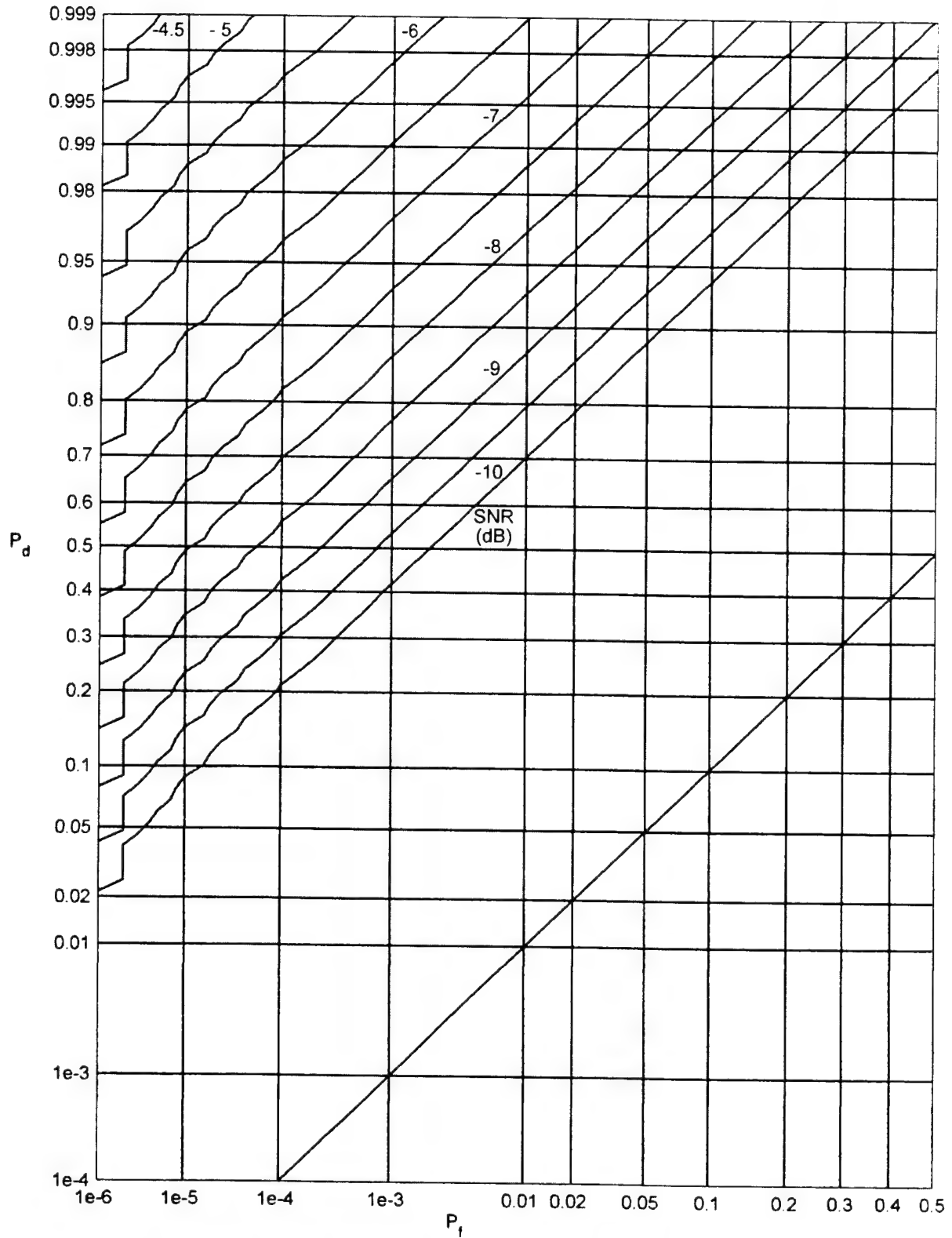


Figure 13. ROCs for Sech Signal in Sech Noise, Processor S

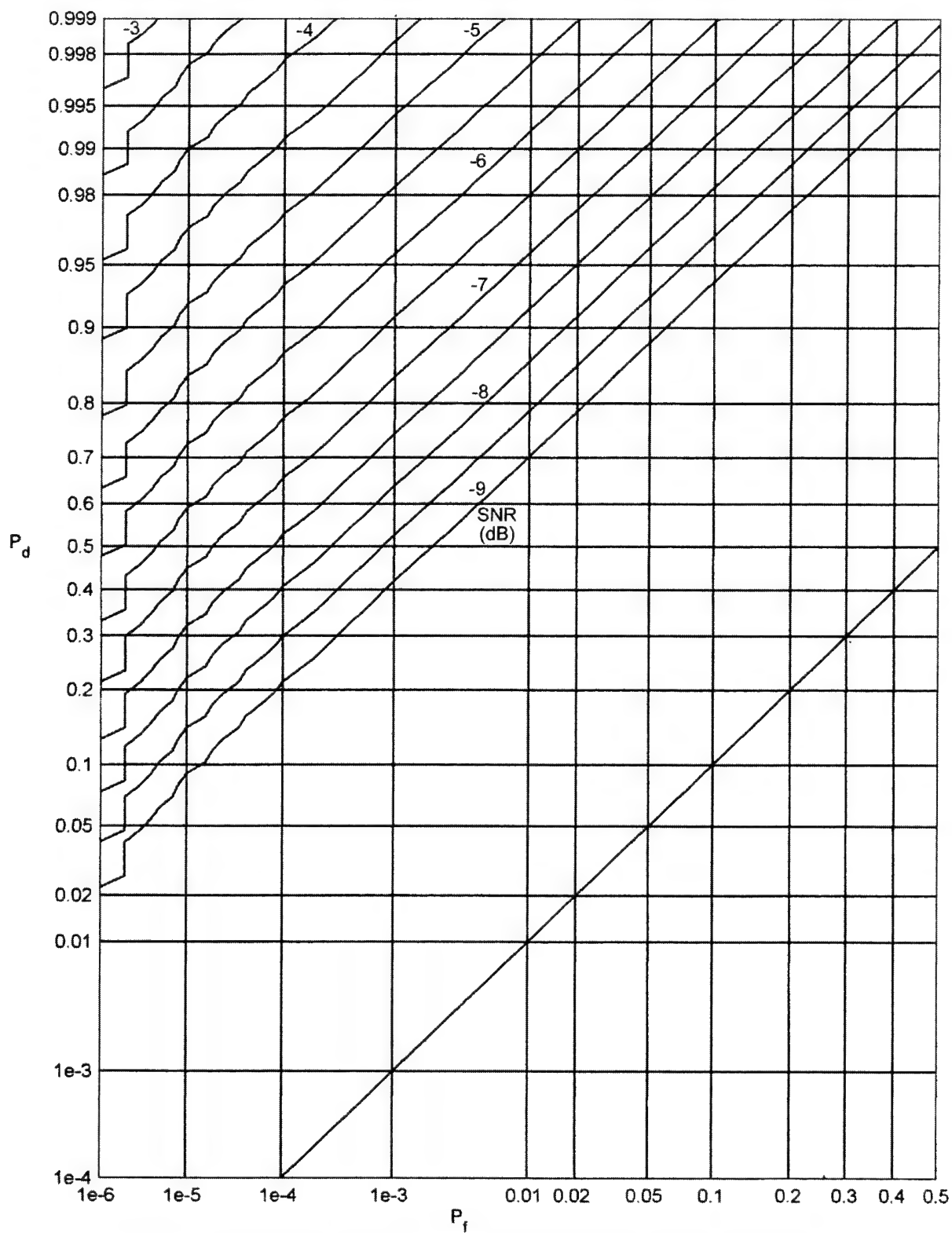


Figure 14. ROCs for Fourth-Power Signal in Sech Noise, Processor S

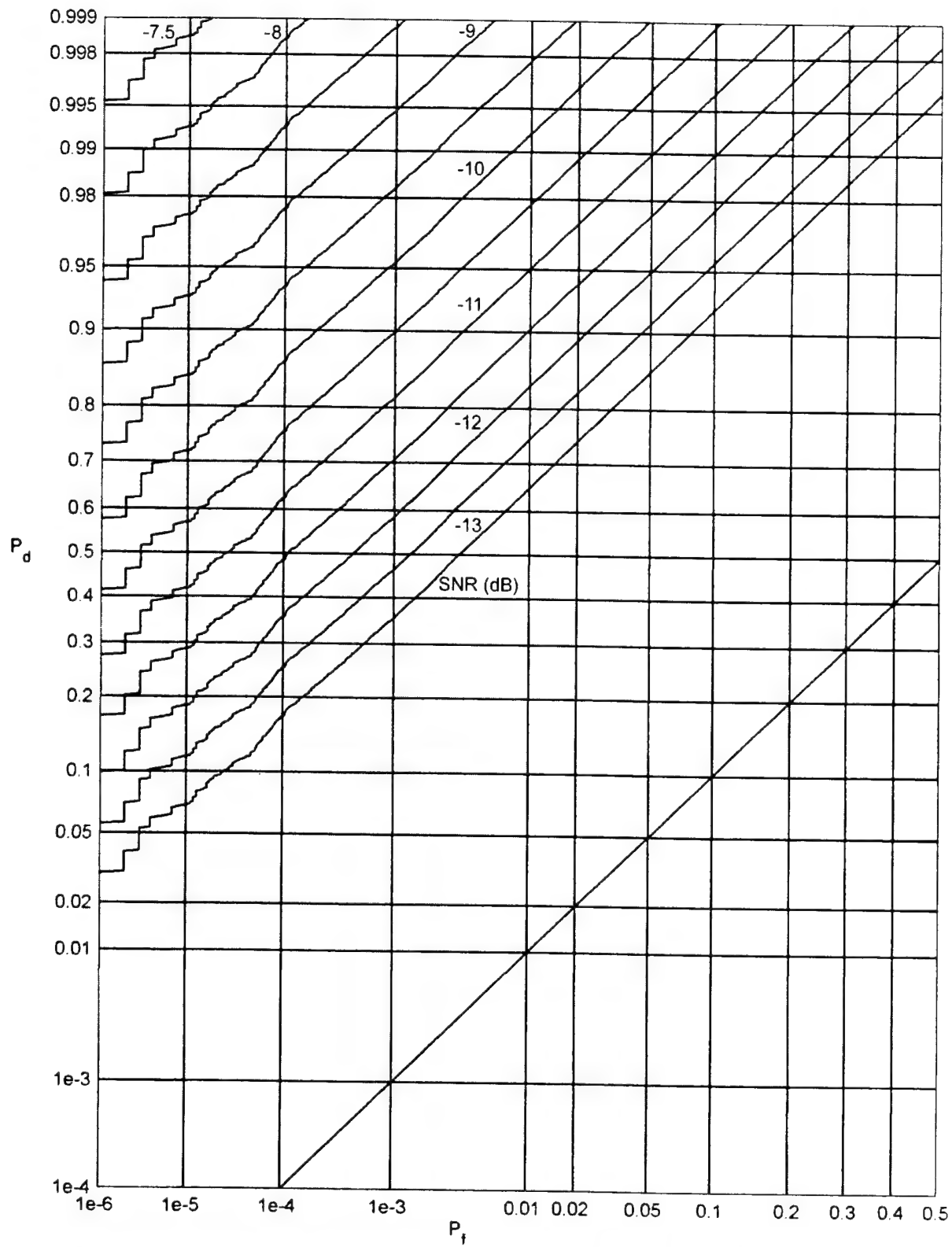


Figure 15. ROCs for Gaussian Signal in Fourth-Power Noise, Processor F

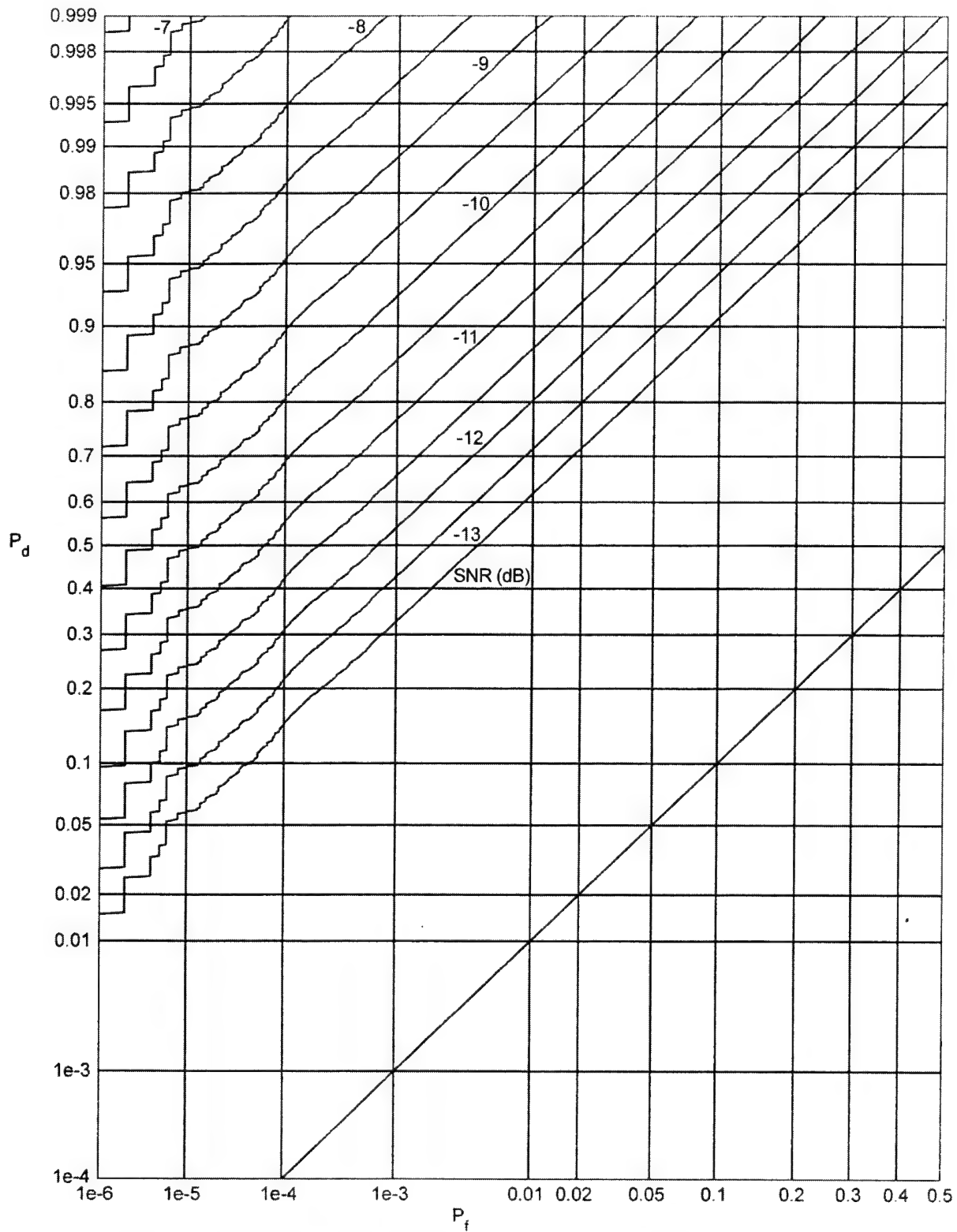


Figure 16. ROCs for Sech Signal in Fourth-Power Noise, Processor F

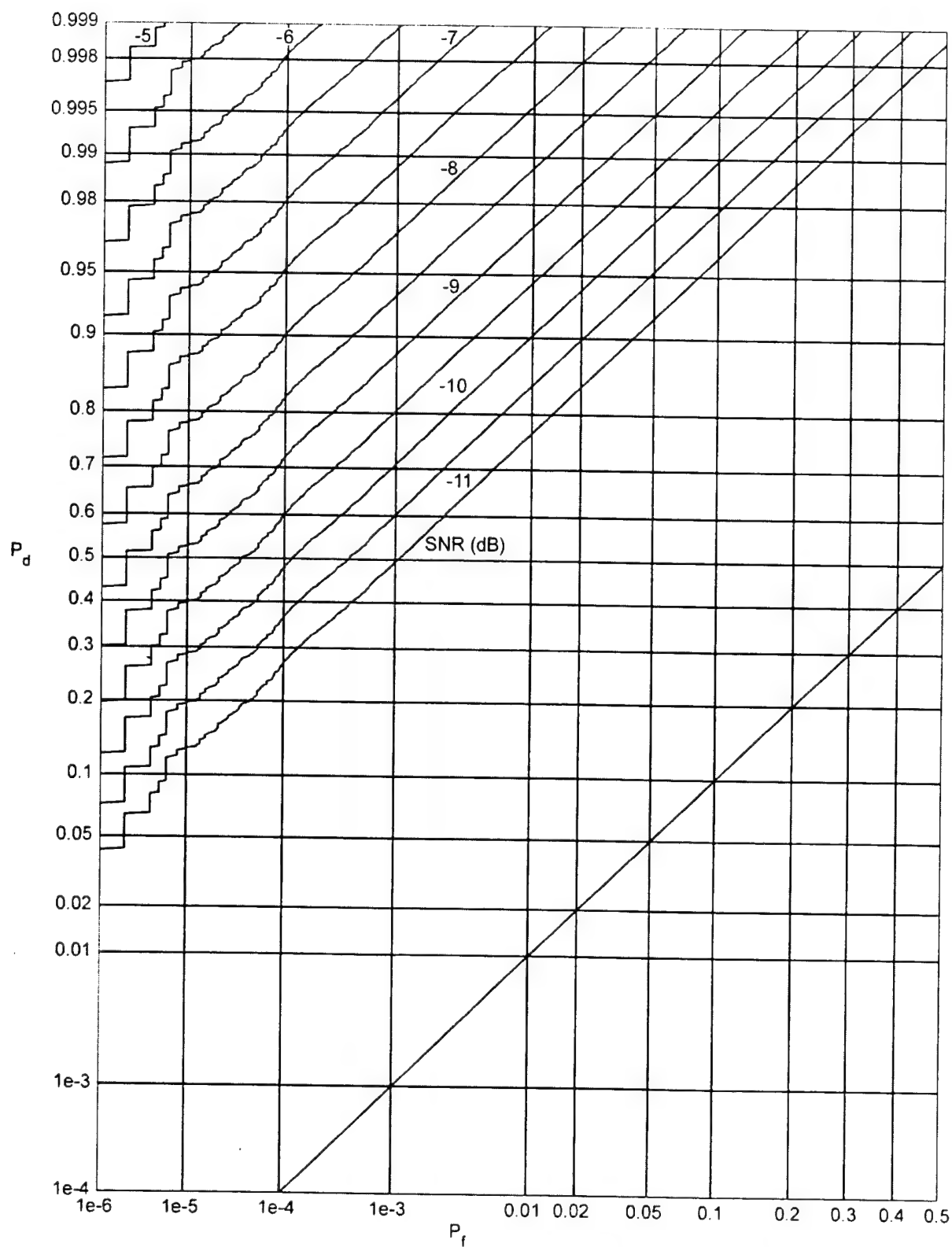


Figure 17. ROCs for Fourth-Power Signal in Fourth-Power Noise, Processor F

DERIVATION OF SUBOPTIMUM PROCESSORS

The form of the optimum processor was presented in equation (1) and is repeated here:

$$\mathbf{L} = \sum_{k=1}^K q''(\mathbf{x}_k) + \sum_{k,j=1}^K \rho_{kj} q'(\mathbf{x}_k) q'(\mathbf{x}_j). \quad (45)$$

Its realization requires knowledge of nonlinearities q' and q'' and the signal normalized covariance matrix ρ . An alternative expression follows as

$$\mathbf{L} = \sum_{k=1}^K q''(\mathbf{x}_k) + \sum_{k=1}^K q'(\mathbf{x}_k)^2 + \sum_{\substack{k,j=1 \\ k \neq j}}^K \rho_{kj} q'(\mathbf{x}_k) q'(\mathbf{x}_j). \quad (46)$$

All the off-diagonal terms in equation (46) require information about the signal characteristics. In the absence of this signal knowledge, dropping these terms suggests a much simpler but suboptimum processor, namely,

$$\mathbf{L}_1 \equiv \sum_{k=1}^K q''(\mathbf{x}_k) + \sum_{k=1}^K q'(\mathbf{x}_k)^2 = \sum_{k=1}^K (q''(\mathbf{x}_k) + q'(\mathbf{x}_k)^2). \quad (47)$$

The degradation of performance caused by this significant reduction depends on the detailed signal characteristics and the particular background noise statistics.

The difficulty of accurately estimating the q' and q'' functions from limited amounts of noise-alone data also begs for some approximation of the nonlinearities indicated in equation (47). A clue to a possible simplification is afforded by the sech noise results in the third line of equation (12). Namely, q'' is the square of q' ; the additive constant can be dropped since it does not affect the ROCs. Furthermore, the second line of equation (12), along with figure 2, indicates that q' is a soft limiter. That is, the suboptimum processor in equation (47) can reasonably be replaced by a soft limiter followed by an energy detector:

$$\mathbf{L}_2 \equiv \sum_{k=1}^K \mathbf{y}_k^2, \quad \mathbf{y}_k = \pm \tanh\left(\frac{\pi}{2} \frac{\mathbf{x}_k}{\sigma}\right) \quad \text{for } k = 1 : K. \quad (48)$$

(The polarity of \mathbf{y}_k is immaterial, because it is squared before summation.) Notice that knowledge of the noise standard deviation σ is needed for realization of processor (48).

More generally, inspection of figures 2, 3, and 5 through 8 reveals that the general behavior of nonlinearity q' is that of a soft limiter, while that of q'' is similar to the square of q' , less an additive constant. This suggests still a further simplification to the suboptimum processor, namely, a hard limiter followed by energy detection:

$$\mathbf{L}_3 \equiv \sum_{k=1}^K \mathbf{y}_k^2, \quad \mathbf{y}_k = \begin{cases} \mathbf{x}_k & \text{for } |\mathbf{x}_k| < b \\ b \operatorname{sgn}(\mathbf{x}_k) & \text{for } |\mathbf{x}_k| > b \end{cases} \quad \text{for } k = 1 : K. \quad (49)$$

The parameter b must be chosen proportional to the noise standard deviation σ to realize the best detectability performance. (This operation is distinct from clipping, for which $\operatorname{sgn}(\mathbf{x}_k)$ would be used for all arguments.) The overall effect of the hard limiting and squaring is equivalent to subjecting the input data samples $\{\mathbf{x}_k\}$ to a squaring operation and saturation:

$$\mathbf{L}_3 = \sum_{k=1}^K \mathbf{z}_k, \quad \mathbf{z}_k = \begin{cases} \mathbf{x}_k^2 & \text{for } |\mathbf{x}_k| < b \\ b^2 & \text{for } |\mathbf{x}_k| > b \end{cases} \quad \text{for } k = 1 : K. \quad (50)$$

Finally, since additive constants do not affect the ROCs, this processor can be modified to

$$\mathbf{L}_4 \equiv \sum_{k=1}^K \mathbf{w}_k, \quad \mathbf{w}_k = \begin{cases} \mathbf{x}_k^2 - b^2 & \text{for } |\mathbf{x}_k| < b \\ 0 & \text{for } |\mathbf{x}_k| > b \end{cases} = \min(\mathbf{x}_k^2 - b^2, 0) \quad \text{for } k = 1 : K. \quad (51)$$

This nonlinearity applied to the input data is simply a negative parabolic bump centered about the origin, and zero for input magnitudes greater than b . Reconsideration of figures 2, 3, and 5 through 8 reveals that is a very reasonable approximation to the function q'' . Furthermore, processor \mathbf{L}_4 has been deduced through an argument that employed a plausible and physically reasonable processor in HT noise, namely, hard limiting followed by energy detection. This argument also lends physical interpretation to the q'' term in optimum processor (1). The only noise parameter that must be monitored is the noise standard deviation; this is a much simpler and stable task than estimating the entire second derivative of the noise PDF. How well this suboptimum processor performs in HT noise distributions must now be determined by simulations.

PERFORMANCE OF A SUBOPTIMUM PROCESSOR

The first case of interest is suboptimum processor (51) for a sech noise background. The ratio of saturation parameter b to the noise standard deviation σ is denoted by ratio

$$r = \frac{b}{\sigma}. \quad (52)$$

Through trial and error, the best value of ratio r , when the background is sech noise, was found to be approximately 1, regardless of the signal type. This value of r maximized the detection probability P_d for a given false alarm probability P_f . The signal model is the same as that described in equation (44) and the accompanying discussion. The ROCs for Gaussian, sech, and fourth-power signals in sech noise are presented in figures 18 through 20, respectively. The losses of this suboptimum processor relative to the optimum results in figures 12 through 14 are given in table 1.

Table 1. Losses of Suboptimum Processor in Sech Noise

Signal Type	Losses (dB)		
Gaussian	1.0	0.95	0.95
Sech	1.0	0.95	0.85
Fourth Power	1.05	1.0	1.0

These are *very* slight losses in detectability, considering the facts that the signal structure is ignored by suboptimum processor (51) and that the noise nonlinearities q' and q'' were not estimated or employed. In fact, the uniformity of the losses over the range of signal statistics (three very different types) and the range of operating points (three widely differing qualities) is surprising.

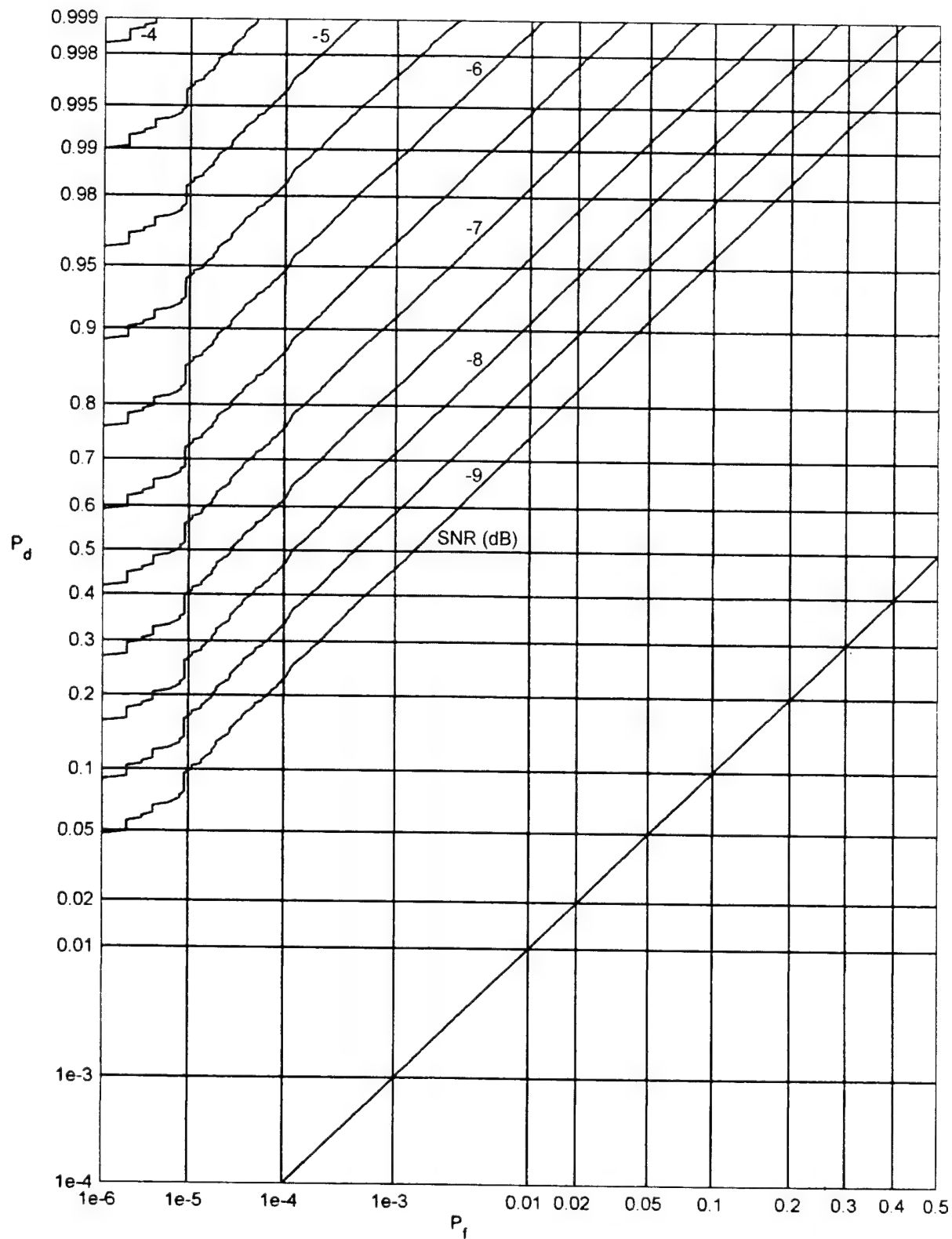


Figure 18. ROCs for Gaussian Signal in Sech Noise, $r = 1.0$

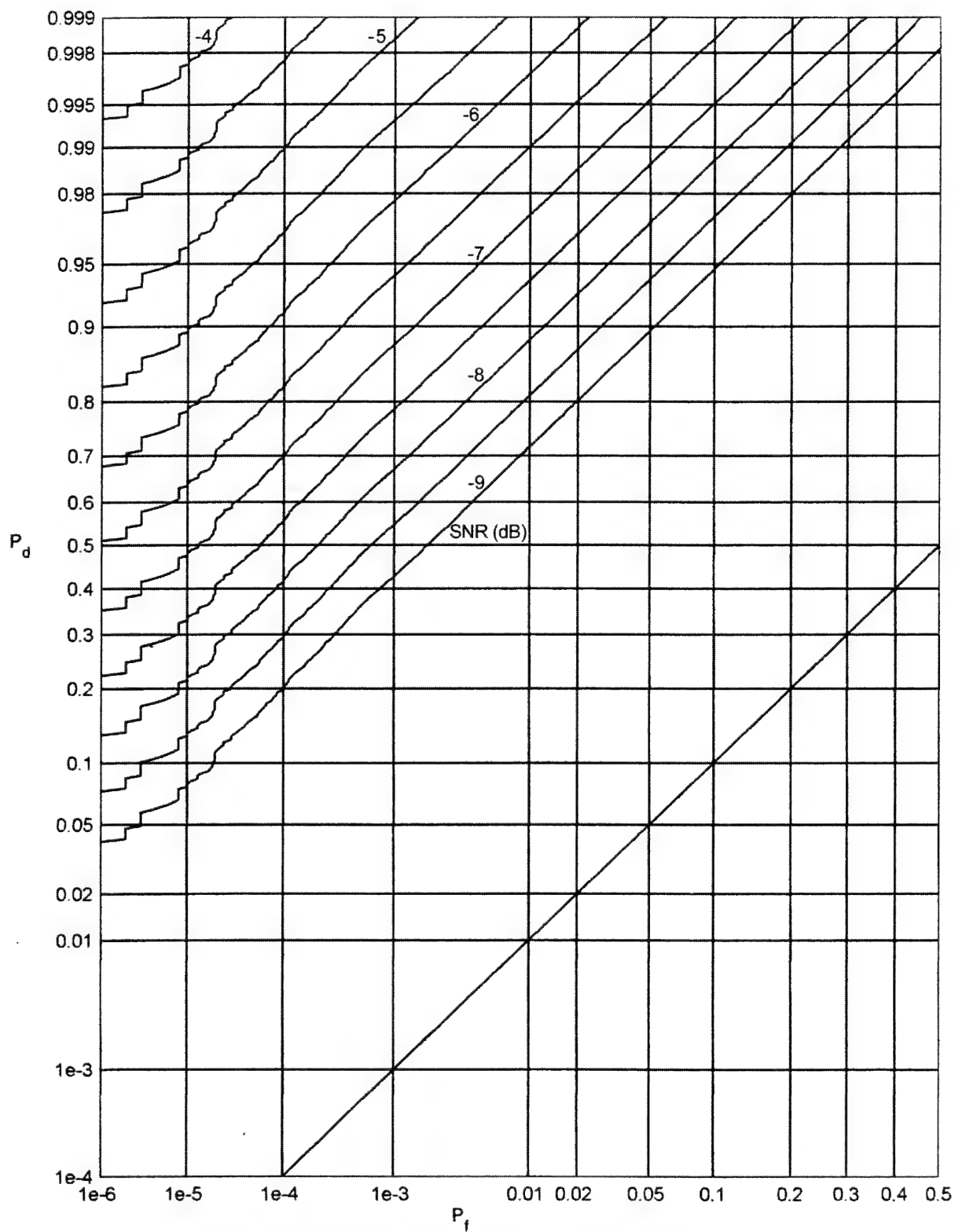


Figure 19. ROCs for Sech Signal in Sech Noise, $r = 1.0$

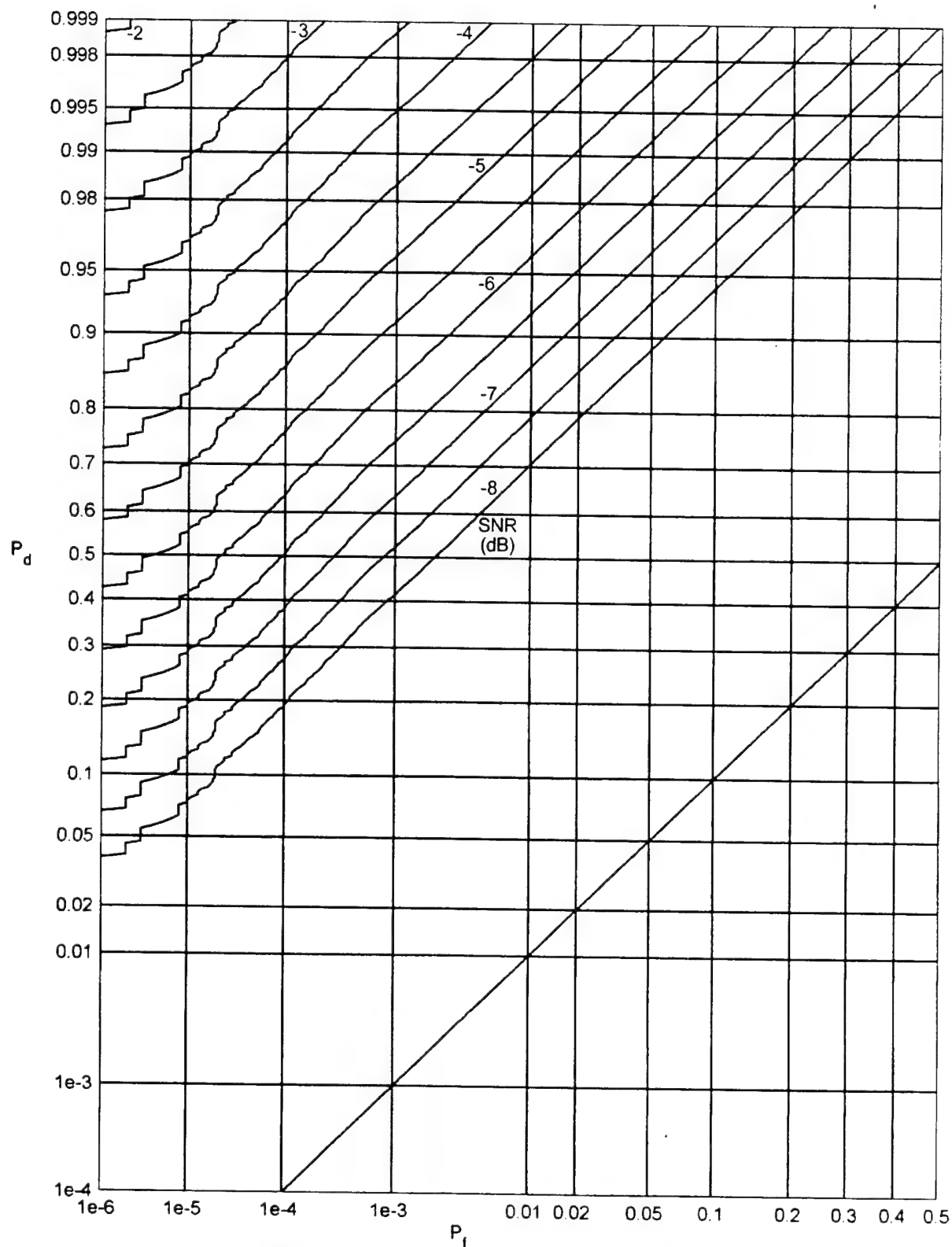


Figure 20. ROCs for Fourth-Power Signal in Sech Noise, $r = 1.0$

The corresponding ROCs for fourth-power noise are presented in figures 21 through 23. Here, the best value of ratio r in equation (52) was found to be approximately 0.65, regardless of the signal type. The losses of the suboptimum processor (51) relative to the optimum results in figures 15 through 17 are given in table 2.

Table 2. Losses of Suboptimum Processor in Fourth-Power Noise

Signal Type	Losses (dB)		
	0.8	0.8	0.8
Gaussian	0.8	0.8	0.8
Sech	0.9	0.85	0.7
Fourth Power	0.8	0.7	0.5

The losses for fourth-power noise are *less* than those for sech noise in table 1. However, the results in table 2 are slightly more variable with regard to signal type and quality of the operating point. Nevertheless, the overwhelming feature of tables 1 and 2 is the relatively insignificant losses associated with employment of suboptimum processor (51). Furthermore, this comparison has been made with the absolute optimum processor (1), which requires knowledge of the detailed signal structure; this signal knowledge will usually not be known in sufficient detail to make much use of it in practice.

Several additional values of ratio r in equation (52) were simulated in addition to the value 0.65 cited above for fourth-power noise. The ROCs were not very sensitive to the exact value of r employed. An example for $r = 0.75$ is given in figure 24; the performance is only slightly poorer than in figure 21. However, the excessive simulation time required to try the various r values prompted the consideration of a simpler detectability measure. In appendix B, the deflection criterion is investigated for Gaussian, sech, and fourth-power noise and suboptimum processor (51). The numerical results on the deflection criterion confirm the choices for r made above with respect to the ROCs themselves. This alternative approach in appendix B can be used to set the ratio r "on the fly" in a practical setting where lengthy ROCs could not be computed.

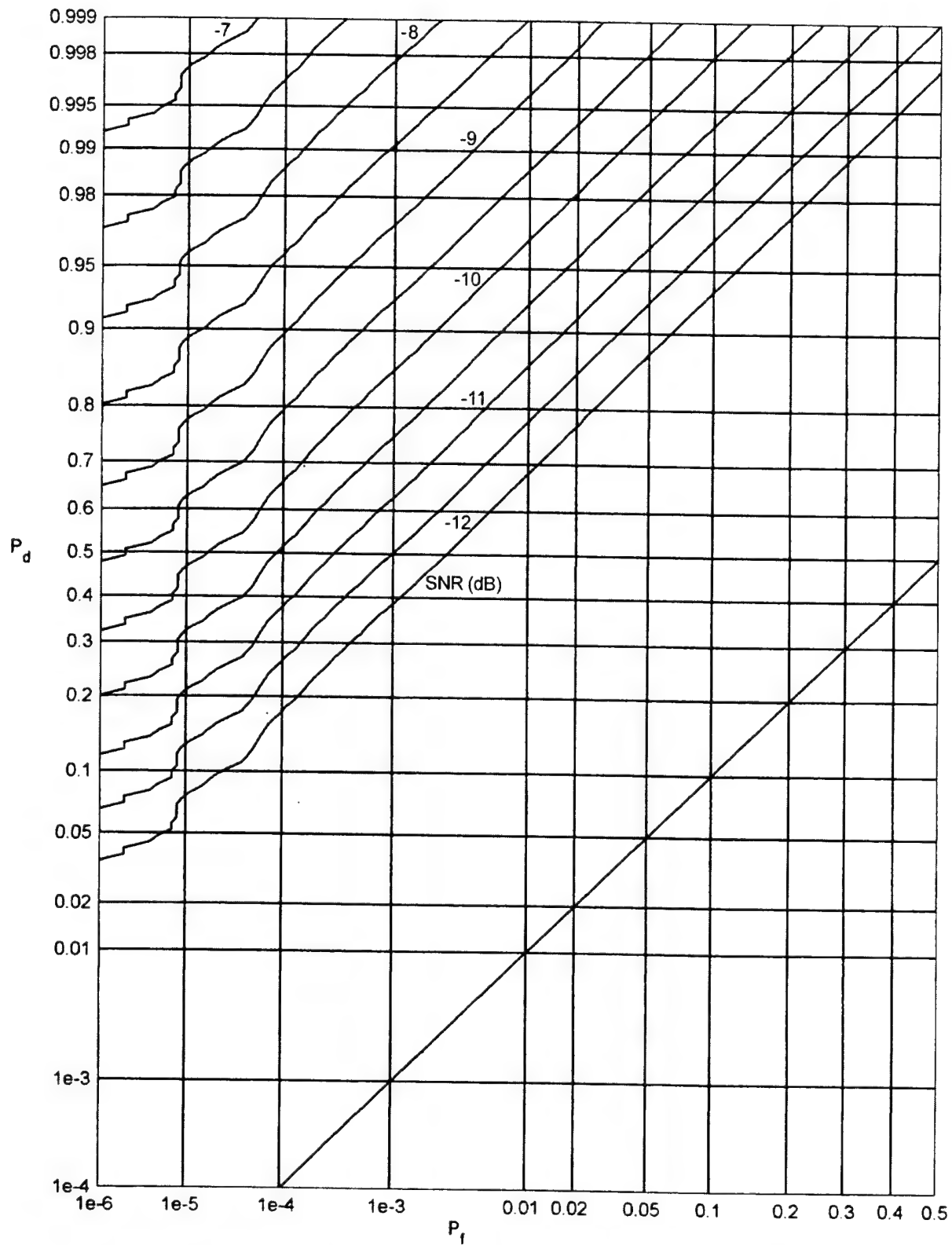


Figure 21. ROCs for Gaussian Signal in Fourth-Power Noise, $r = 0.65$

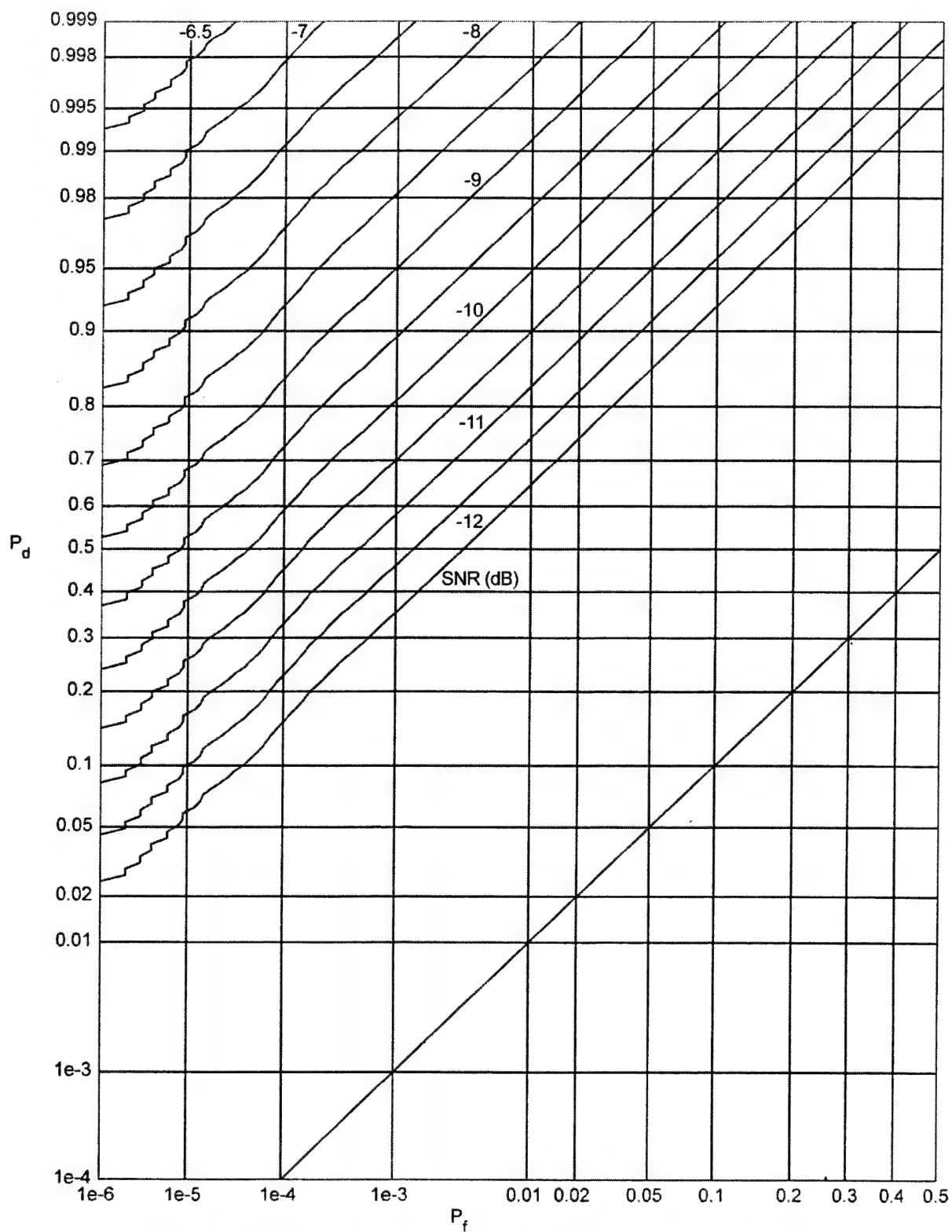


Figure 22. ROCs for Sech Signal in Fourth-Power Noise, $r = 0.65$

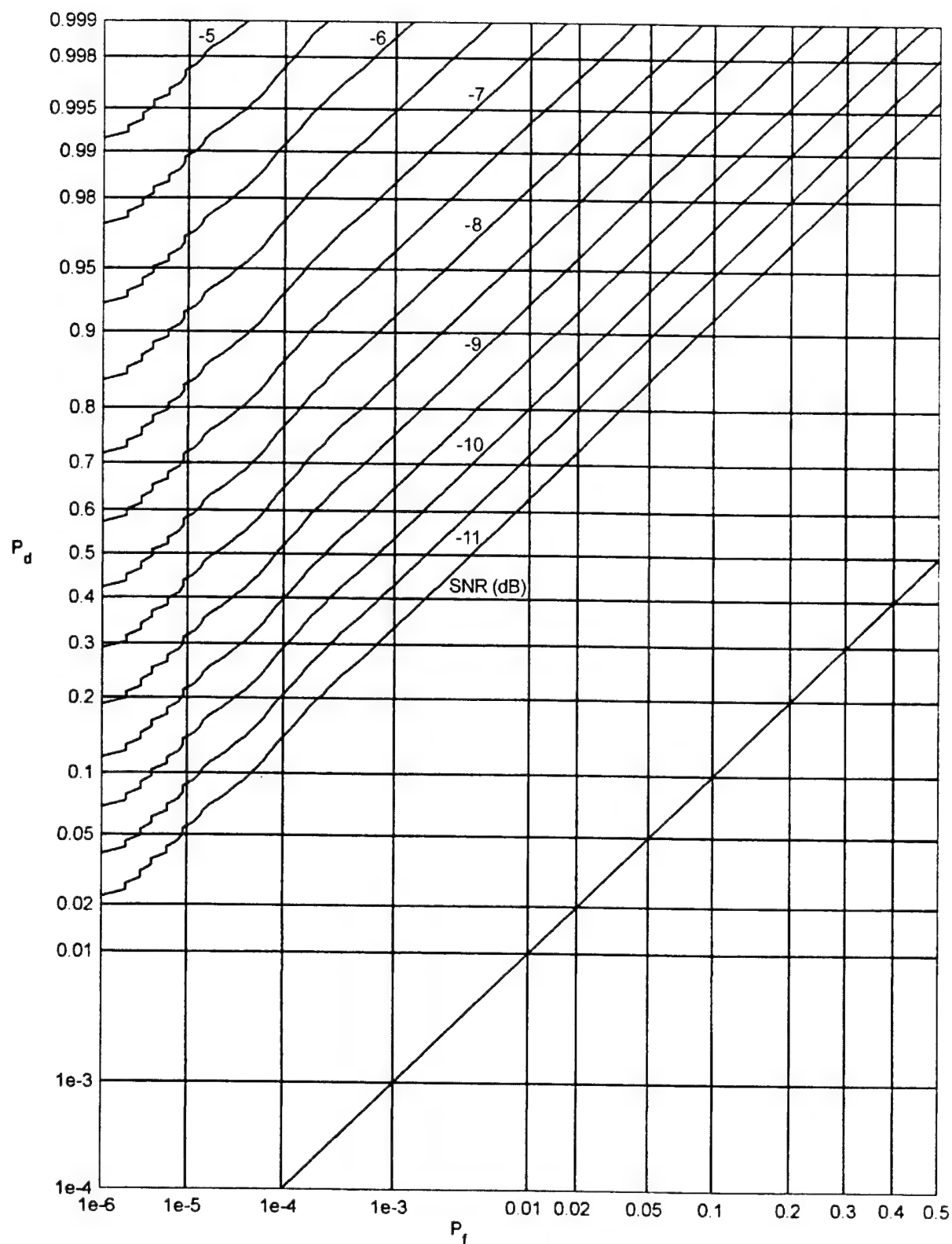


Figure 23. ROCs for Fourth-Power Signal in Fourth-Power Noise, $r = 0.65$

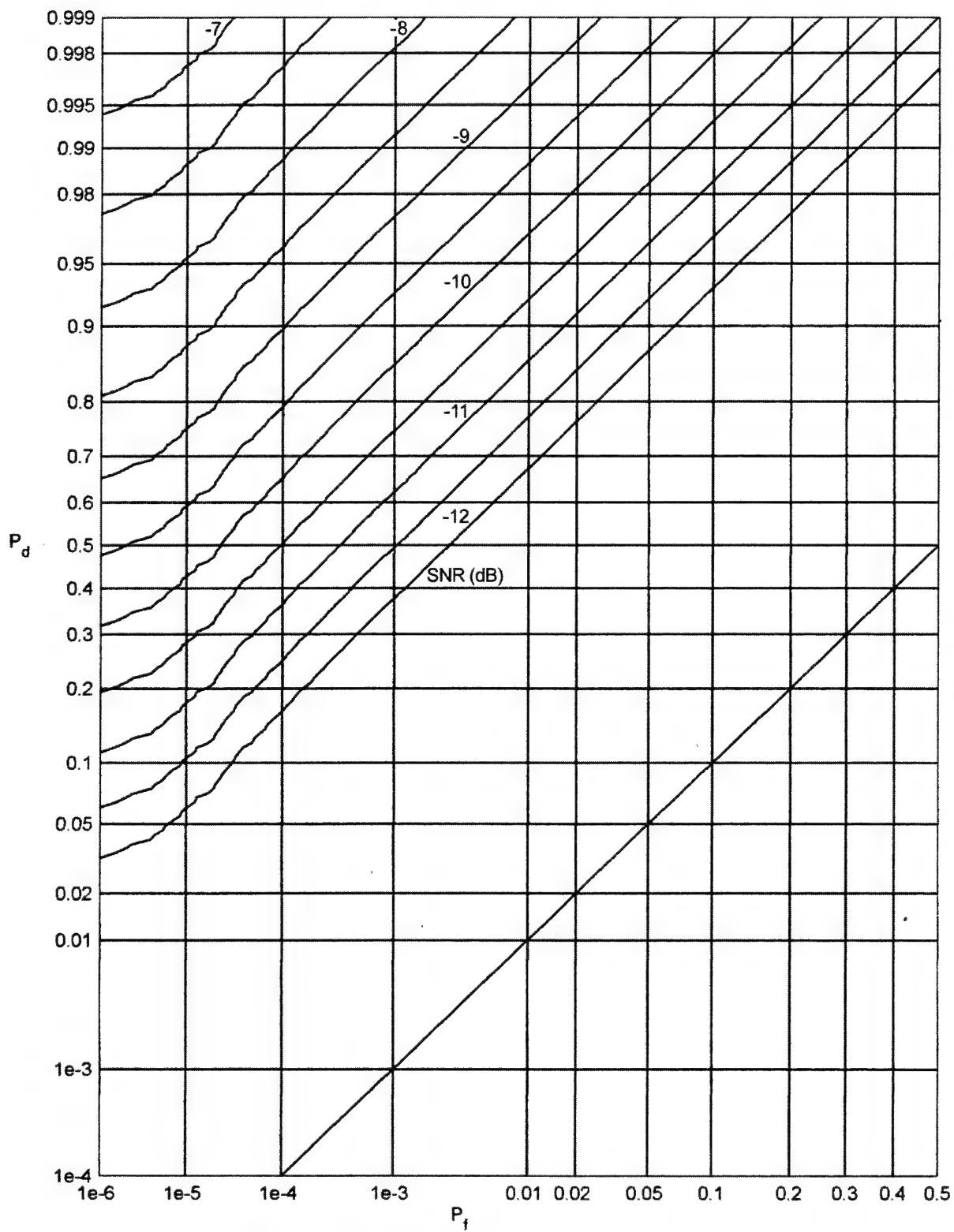


Figure 24. ROCs for Gaussian Signal in Fourth-Power Noise, $r = 0.75$

Thus far, the signal model has been that of equation (44) with relative attenuation factor $\alpha = -1$ and $m = 10$. To ascertain the dependence on the signal structure, the factor α is now set equal to -0.5 . The received signal is Gaussian and the background is maintained as fourth-power noise. The ROCs for the optimum processor are presented in figure 25, while those for the suboptimum processor are displayed in figure 26. When factor α is set to zero (no surface reflection, making m irrelevant), the corresponding ROCs for the optimum and suboptimum processors are given in figures 27 and 28, respectively.

The dependencies of the detectability losses of the suboptimum processor relative to the optimum processor are listed in table 3. The top line comes from table 2, while the bottom two lines come from figures 25 through 28. The three numbers on a line correspond to the low-, medium-, and high-quality OPs, respectively. Two features stand out: the variation with OP is virtually nil, and the degradation with respect to relative attenuation factor α decreases to zero as α does. This is not precisely true; however, there is very little difference between the ROCs in figures 27 and 28.

Table 3. Dependence of Losses on Signal Structure

α	Losses (dB)		
-1.0	0.8	0.8	0.8
-0.5	0.6	0.5	0.4
0.0	0	0	0

Finally, a signal with *more* structure, rather than less, was considered. Signal model (44) was expanded to include three paths with relative strengths $+1, -1, +1$ and delays 0, 10, 20, respectively. The ROCs for the corresponding optimum processor are given in figure 29, while the ROCs for the suboptimum processor are given in figure 30. Now the loss is a uniform 1.5 dB across all the OPs. This loss is greater than any of those encountered in tables 1 through 3 and is due to the increased off-diagonal structure of the signal covariance matrix. This increasing loss can be expected to prevail as the off-diagonal structure increases in complexity. However, the likelihood of knowing this information in advance is not reasonable in practice. Therefore, the relatively small losses listed above must be taken as extremely encouraging in detection of a weak signal in HT noise.

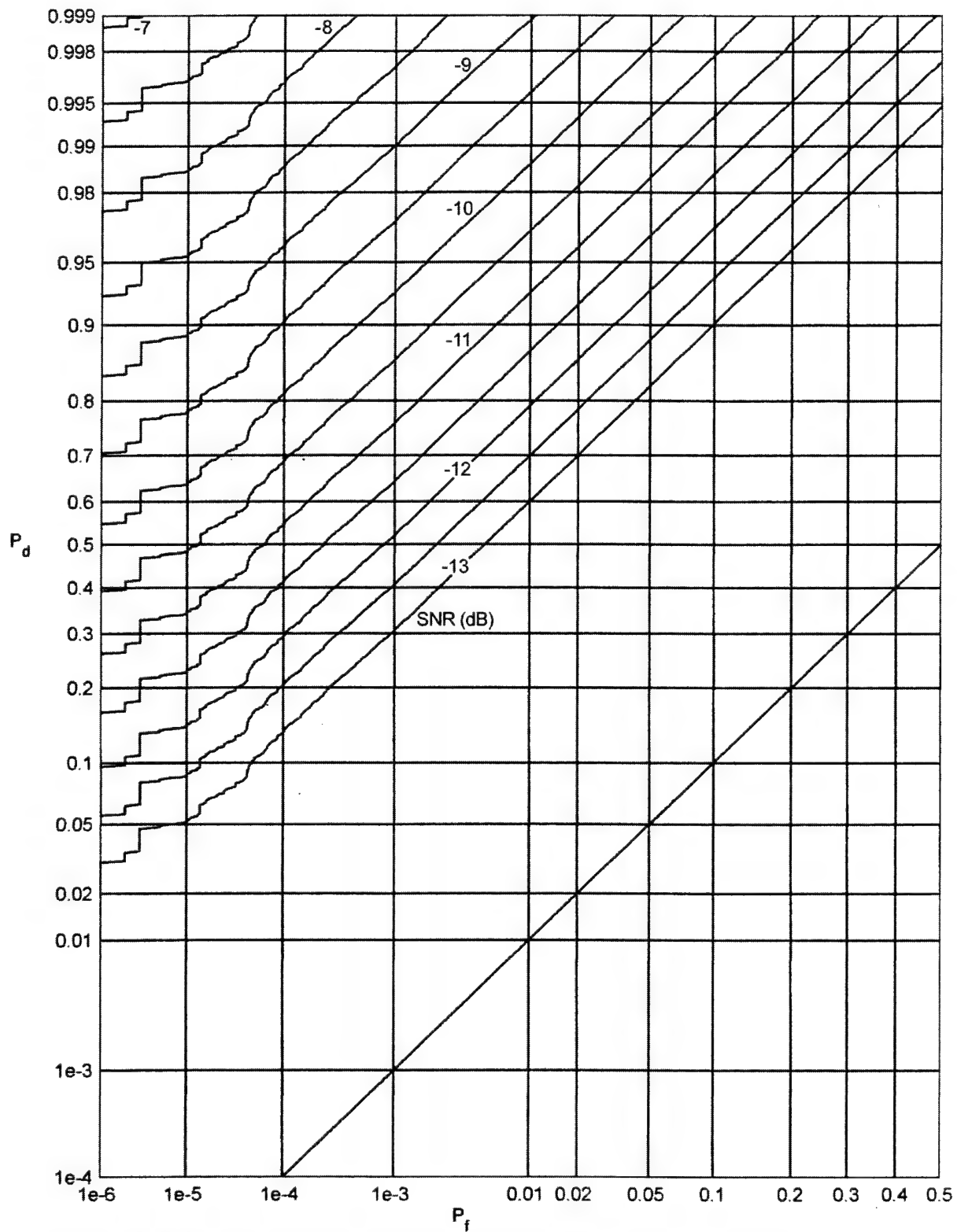


Figure 25. ROCs for Gaussian Signal in Fourth-Power Noise, Processor F, $\alpha = -0.5$

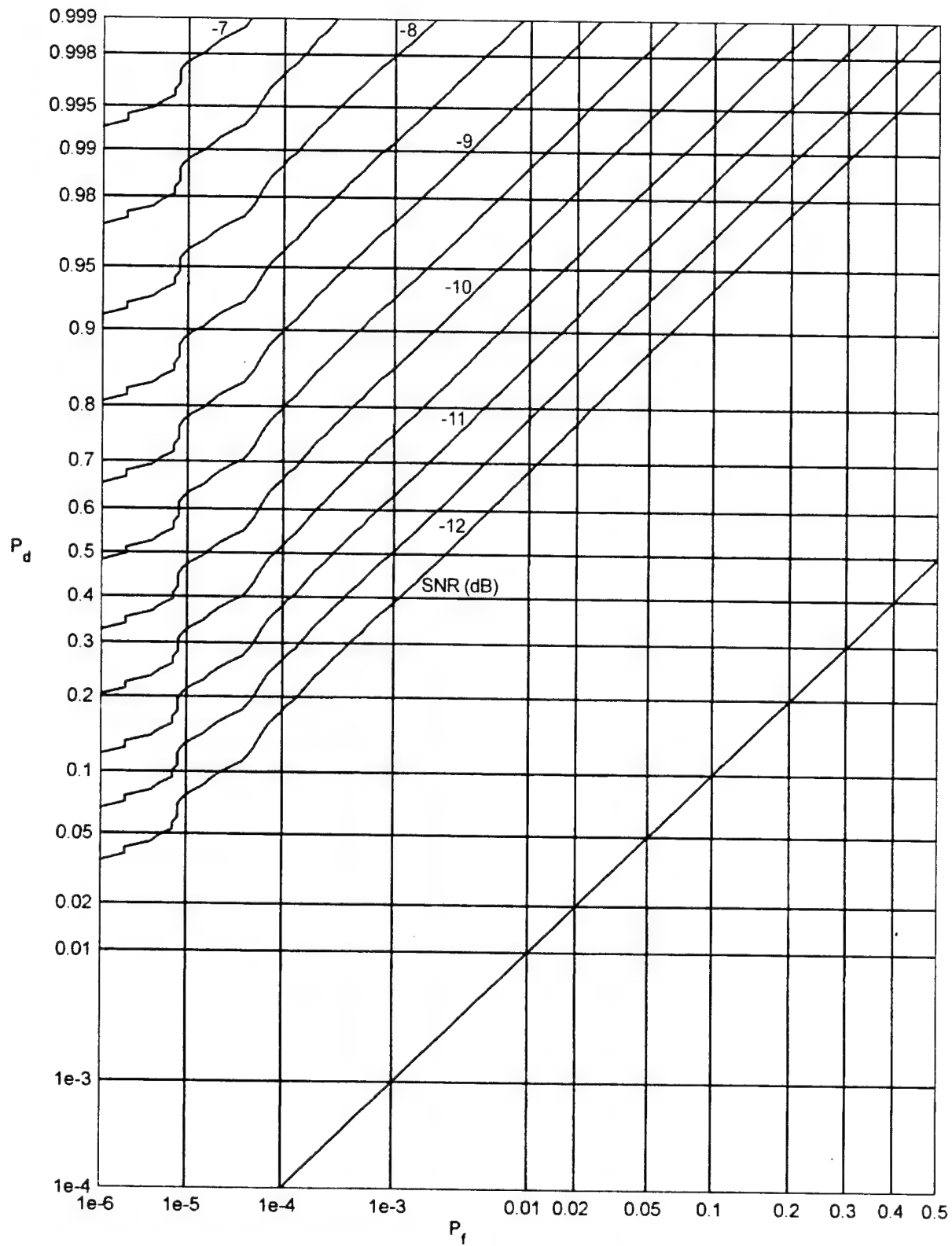


Figure 26. ROCs for Gaussian Signal in Fourth-Power Noise, $r = 0.65$, $\alpha = -0.5$

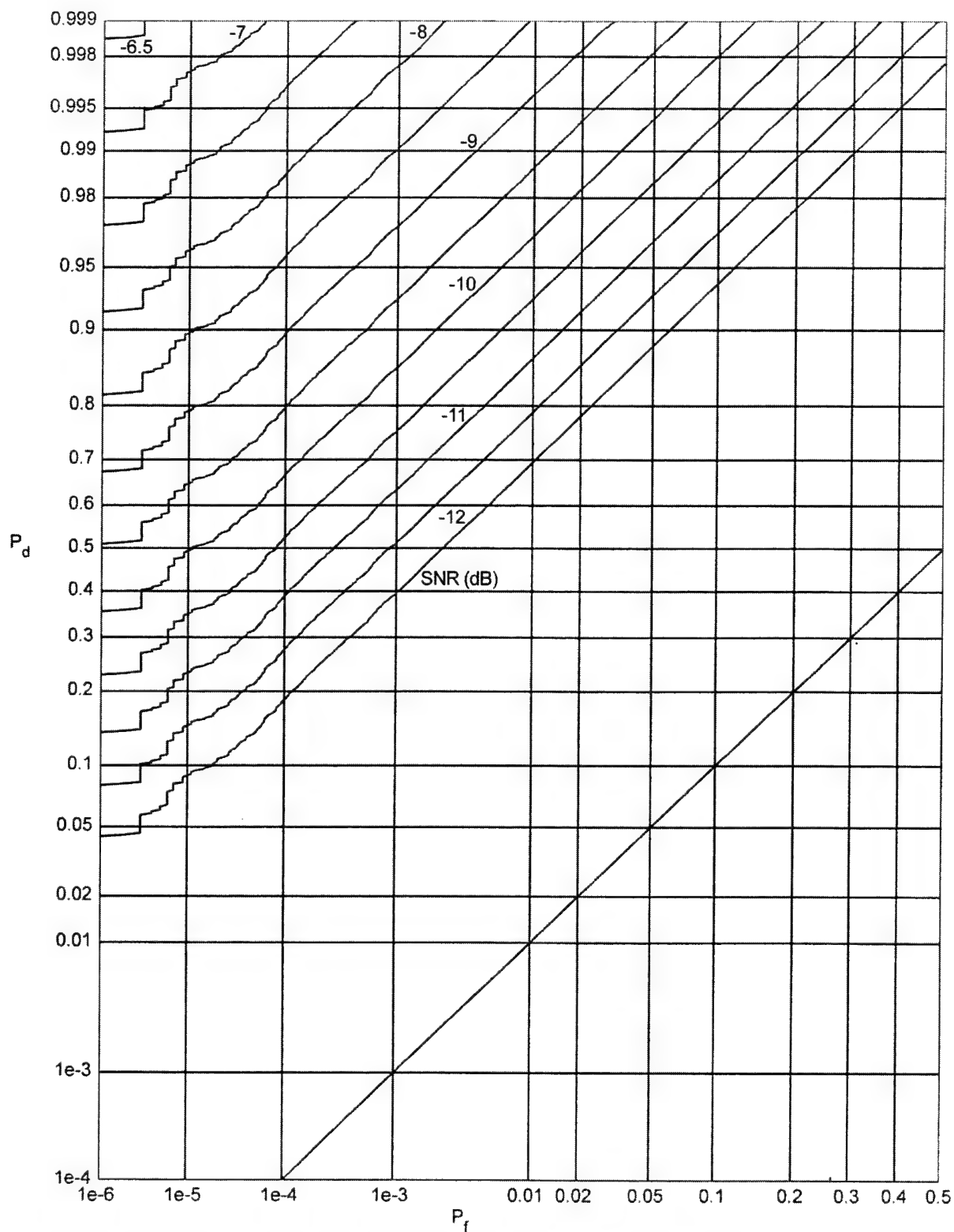


Figure 27. ROCs for Gaussian Signal in Fourth-Power Noise, Processor F, $\alpha = 0.0$

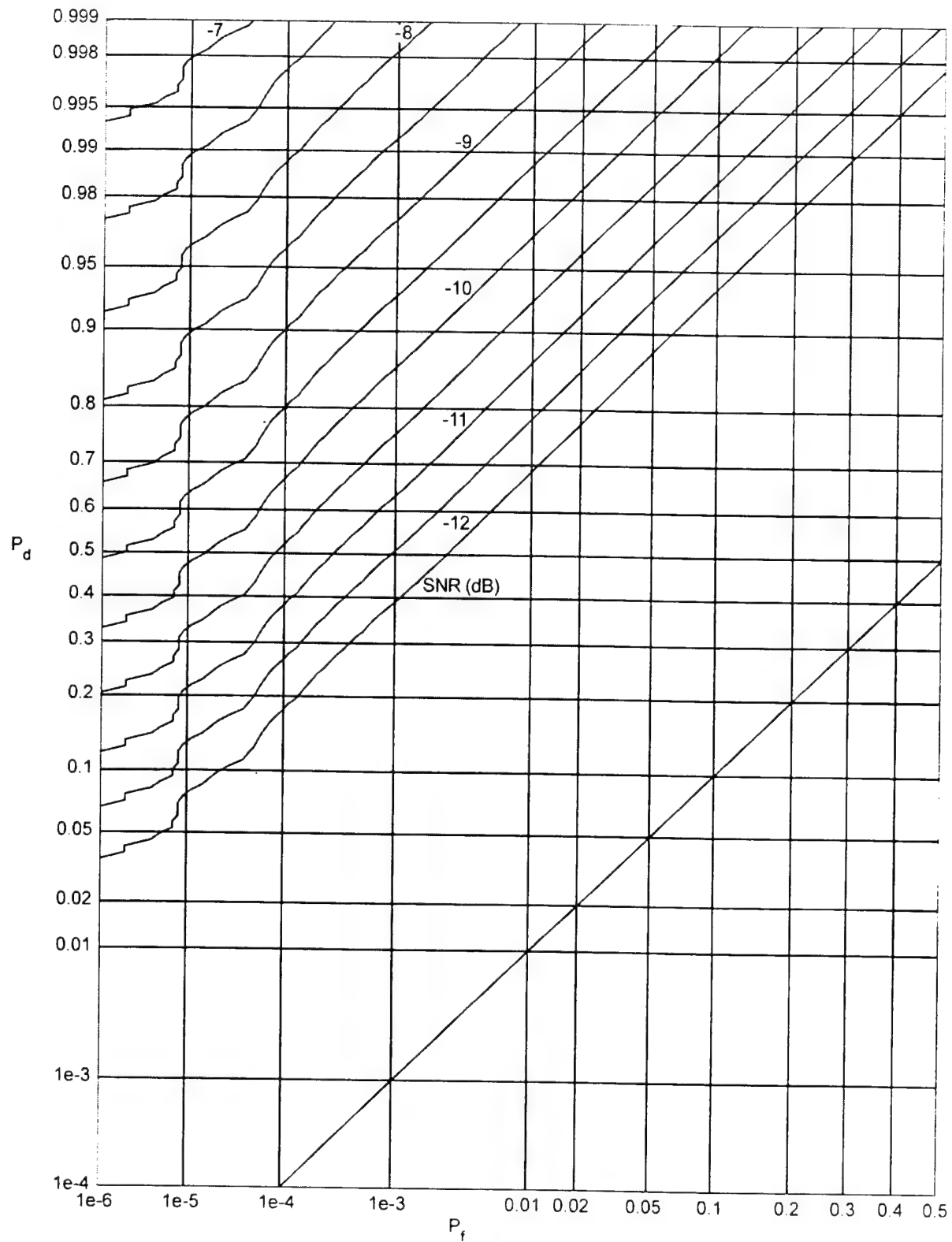


Figure 28. ROCs for Gaussian Signal in Fourth-Power Noise, $r = 0.65$, $\alpha = 0.0$

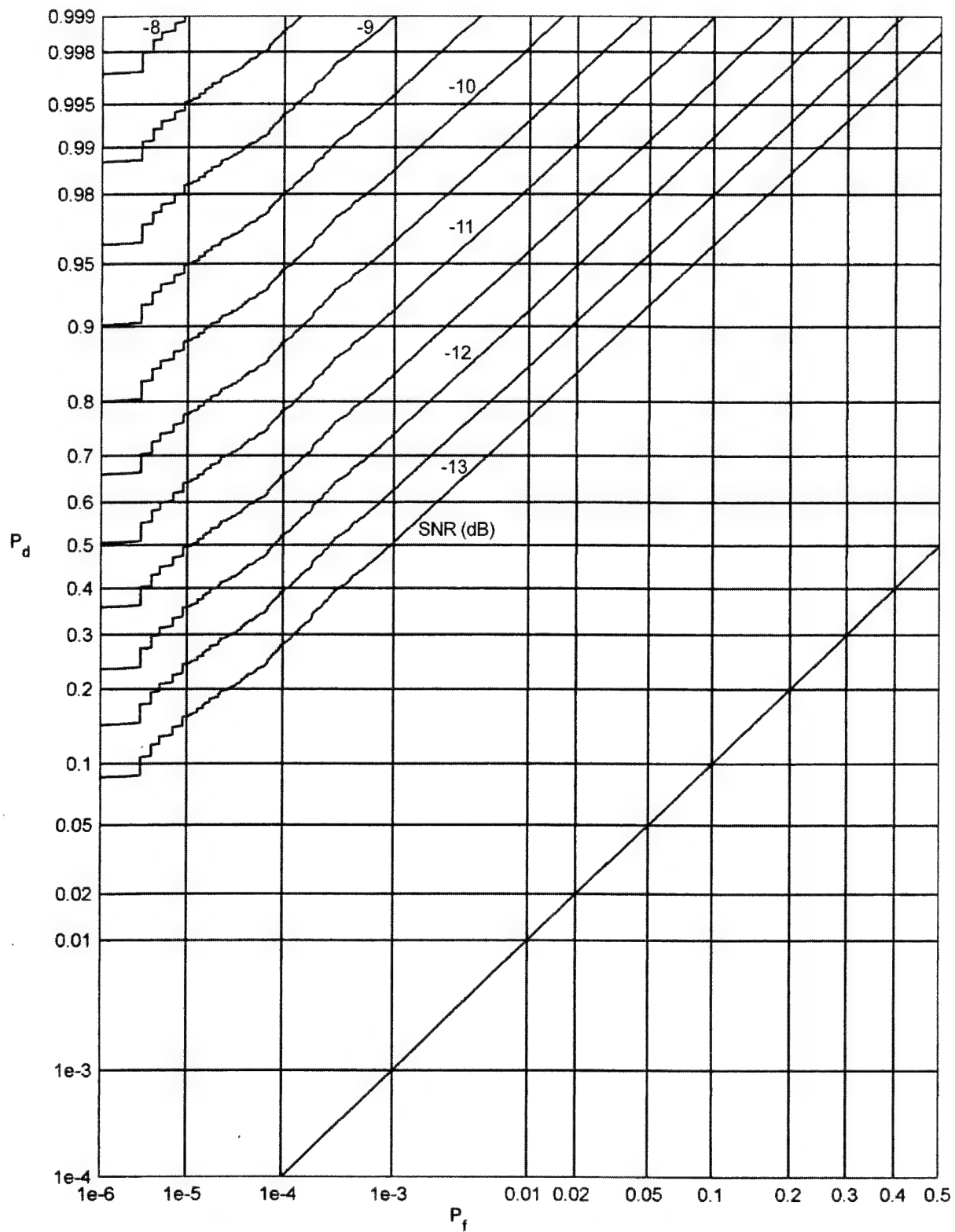


Figure 29. ROCs for Gaussian Signal in Fourth-Power Noise, Processor F, $\alpha = [-1, 1]$

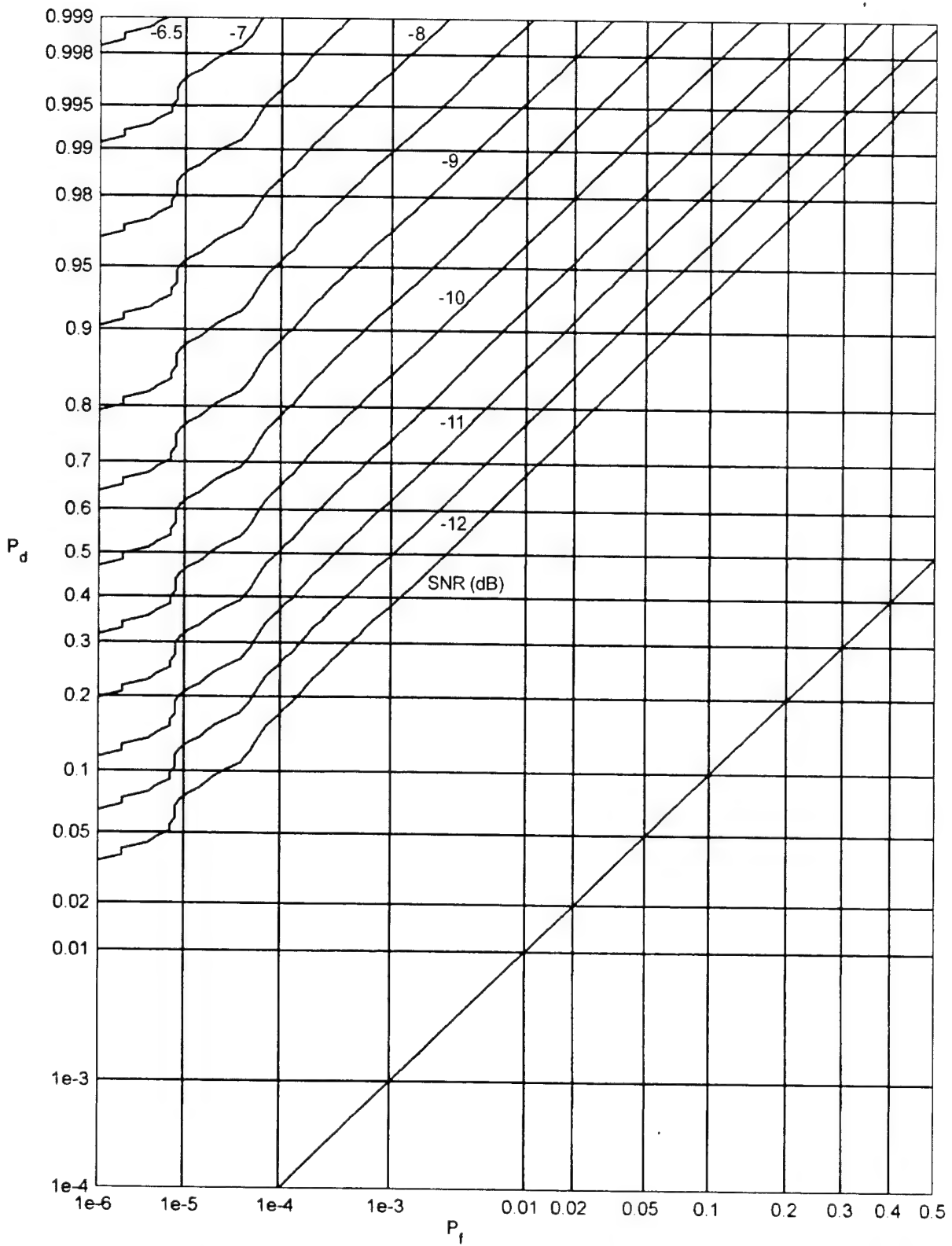


Figure 30. ROCs for Gaussian Signal in Fourth-Power Noise, $r = 0.65$, $\alpha = [-1, 1]$

SUMMARY

The optimum processor has been derived for optimum detection of a weak stationary signal with multipath in the presence of additive non-Gaussian noise. The optimum processor requires knowledge of the signal normalized covariance matrix and the first two derivatives of the first-order probability density function of the noise. The difficulty in obtaining some or all of this information in practice suggests alternative simpler processors that require only partial or minimal information for their realization. However, these alternative processors have degraded detection capability relative to the optimum processor, and the exact amounts of these losses are important and must be determined before any alternatives can be considered acceptable.

A particular suboptimum processor has been investigated here, namely, a hard limiter followed by an energy detector. The hard limiter prevents the heavy-tailed noise contributions from reaching the processor output, while the long-term energy detection allows for the weak signal (if present) to contribute to the device output, enabling its detection even in low input signal-to-noise ratio situations. Signal structure information is ignored by this processor. The losses in performance typically run on the order of 1 dB, regardless of whether low-quality or high-quality detection performance is required. This rather low loss is very encouraging, especially in the presence of heavy-tailed noise distributions, which can lead to catastrophic losses in the usual linear processor designed for a Gaussian background. The plausibility of this type of processor is also confirmed by deriving it as an approximation to the optimum processor.

This quantitative study provides a basis for making some conclusions about operating in a non-Gaussian environment; such studies are few and far between. It has concentrated on accurate evaluation of the receiver operating characteristics of the various processors, thereby furnishing hard numerical signal-to-noise ratio comparisons. The cost of ignoring pertinent information or using inaccurate estimates can be accurately assessed, and further studies can be initiated to gather the pertinent required data, with full knowledge of the gains to be accrued. Also, the ultimate detectability of a signal in that particular non-Gaussian environment can be ascertained, once and for all, for possible future applications.

REFERENCES

1. A. H. Nuttall, "Optimum Detection of Random Signal in Non-Gaussian Noise for Low Input Signal-to-Noise Ratio," NUWC-NPT Technical Report 11,512, Naval Undersea Warfare Center Division, Newport, RI, 23 February 2004.
2. I. S. Gradshteyn and I. M. Ryzhik, *Table of Integrals, Series, and Products*, Academic Press Inc., New York, 1980.
3. *Handbook of Mathematical Functions*, U.S. Department of Commerce, National Bureau of Standards, Applied Mathematics Series, No. 55, U.S. Government Printing Office, Washington, DC, June 1964.

APPENDIX A INVERSION OF CDF FOR FOURTH-POWER RANDOM VARIABLE

The essential problem in inverting equation (22) in the main body of this report for the fourth-power cumulative distribution function (CDF) is the solution of the following equation for x in terms of y :

$$y = 2 \operatorname{atan}(x) - \operatorname{atan}(x/2). \quad (\text{A-1})$$

The appropriate steps follow:

$$y + \operatorname{atan}(x/2) = 2 \operatorname{atan}(x), \quad \tan(y + \operatorname{atan}(x/2)) = \tan(2 \operatorname{atan}(x)). \quad (\text{A-2})$$

Let $z = \tan(y)$. Then, equation (A-2) yields

$$\frac{z + x/2}{1 - z x/2} = \frac{2x}{1 - x^2}, \quad (2z + x)(1 - x^2) = 2x(2 - zx), \quad x^3 + 3x - 2z = 0. \quad (\text{A-3})$$

Let $x = t + u$ to get

$$t^3 + u^3 - 2z + 3(t + u)(1 + tu) = 0. \quad (\text{A-4})$$

Now let $u = -1/t$ to get

$$t^3 - \frac{1}{t^3} - 2z = 0, \quad t^6 - 2zt^3 - 1 = 0, \quad t^3 = z + \sqrt{1 + z^2},$$

$$t = \left(z + \sqrt{1 + z^2} \right)^{1/3} = \exp\left(\frac{1}{3} \log(z + \sqrt{1 + z^2}) \right) = \exp\left(\frac{1}{3} \operatorname{asinh}(z) \right). \quad (\text{A-5})$$

Therefore, the real solution to equation (A-1) is

$$x = t - \frac{1}{t}, \quad t = \left(z + \sqrt{1 + z^2} \right)^{1/3}, \quad z = \tan(y). \quad (\text{A-6})$$

Alternative forms for t directly in terms of y are

$$t = \left(\frac{1 + \sin(y)}{\cos(y)} \right)^{1/3} = \left[\cot\left(\frac{\pi}{4} - \frac{y}{2} \right) \right]^{1/3}. \quad (\text{A-7})$$

The nonlinear transformation that yields zero-mean, unit-variance fourth-power random variables (RVs) \mathbf{x} directly from uniformly distributed RVs \mathbf{u} over (0,1) is given by equation (23) as

$$\mathbf{x} = \sqrt{2} \sinh\left(\frac{1}{3} \log\left(\tan\left(\frac{\pi}{2} \mathbf{u}\right)\right)\right). \quad (\text{A-8})$$

The CDFs and probability density functions (PDFs) of the unit-variance components of this transformation are

$$\begin{aligned} \mathbf{x}_1 &= \tan\left(\frac{\pi}{2} \mathbf{u}\right), \quad c_1(x) = \frac{2}{\pi} \operatorname{atan}(x), \quad p_1(x) = \frac{2/\pi}{1+x^2} \quad \text{for } 0 < x < \infty; \\ \mathbf{x}_2 &= \frac{2}{\pi} \log(\mathbf{x}_1), \quad c_2(x) = \frac{2}{\pi} \operatorname{atan}\left(\exp\left(\frac{\pi}{2} x\right)\right), \quad p_2(x) = \frac{1}{2} \operatorname{sech}\left(\frac{\pi}{2} x\right) \quad \text{for all } x; \\ \mathbf{x} &= \sqrt{2} \sinh\left(\frac{\pi}{6} \mathbf{x}_2\right), \quad c(x) = \frac{2}{\pi} \operatorname{atan}\left(\exp\left(3 \operatorname{asinh}\left(\frac{x}{\sqrt{2}}\right)\right)\right), \\ p(x) &= \frac{3/(\sqrt{2} \pi)}{(1+2x^2)(1+x^2/2)} \quad \text{for all } x. \end{aligned} \quad (\text{A-9})$$

All of the results above and in equations (20) through (24) are special cases of the following equations, when b is set equal to 3. The general CDF is

$$c(x) = \frac{2}{\pi} \operatorname{atan}\left[\left(\frac{x}{a} + \sqrt{1 + \frac{x^2}{a^2}}\right)^b\right] = \frac{2}{\pi} \operatorname{atan}\left(\exp\left(b \operatorname{asinh}\left(\frac{x}{a}\right)\right)\right) \quad \text{for all } x, \quad (\text{A-10})$$

where b need not be integer. Letting $y = c(x)$, the inverse relation is

$$x = \tilde{c}(y) = a \sinh\left(\frac{1}{b} \log\left(\tan\left(\frac{\pi}{2} y\right)\right)\right) \quad \text{for } 0 < y < 1. \quad (\text{A-11})$$

The general PDF is the derivative of equation (A-10); namely,

$$p(x) = \frac{2}{\pi} \frac{b/a}{q} \frac{1}{(q+x/a)^b + (q-x/a)^b}, \quad q \equiv \sqrt{1 + \frac{x^2}{a^2}}, \quad a > 0, \quad b > 0. \quad (\text{A-12})$$

The asymptotic behavior of the PDF is according to the inverse $b+1$ power:

$$p(x) \sim \frac{4}{\pi} \frac{b}{a} \left(\frac{a}{2|x|}\right)^{b+1} \quad \text{as } x \rightarrow \pm\infty. \quad (\text{A-13})$$

Thus, RVs with any desired asymptotic power-law behavior can be generated by means of equation (A-11), when y is replaced by a uniformly distributed RV over (0,1).

For the variance to be finite, that is,

$$\sigma^2 = \int dx x^2 p(x) < \infty, \quad (\text{A-14})$$

the parameter b must be greater than 2. Then,

$$\sigma^2 = a^2 Q(b), \quad (\text{A-15})$$

where

$$Q(b) = \frac{4}{\pi} \int_0^\infty \frac{du}{\sqrt{1+u^2}} \frac{b u^2}{\left(\sqrt{1+u^2} + u\right)^b + \left(\sqrt{1+u^2} - u\right)^b}, \quad b > 2. \quad (\text{A-16})$$

For a given value of b , relations (A-15) and (A-16) give the required value of parameter a ; namely,

$$a = \frac{\sigma}{\sqrt{Q(b)}}, \quad (\text{A-17})$$

in terms of the desired standard deviation σ . The integral in equation (A-16) can be evaluated in closed form for b equal to small integers:

$$Q(3) = \frac{1}{2}, \quad Q(4) = \frac{\sqrt{2}-1}{2}, \quad Q(5) = \frac{\sqrt{5}-2}{2}, \quad Q(6) = \frac{2\sqrt{3}-3}{6}. \quad (\text{A-18})$$

Additional non-integer b values will require numerical integration of equation (A-16). However, one special case that can be evaluated in closed form is $Q(2.5) = \sqrt{5}/2$.

APPENDIX B

DEFLECTION CRITERION FOR SUBOPTIMUM PROCESSOR

The decision variable is given by a sum of K independent samples of noise plus signal (if present) subjected to an arbitrary nonlinear transformation f :

$$\mathbf{w} = \sum_{k=1}^K f(\mathbf{x}_k) \equiv \sum_{k=1}^K \mathbf{y}(k). \quad (\text{B-1})$$

The relevant deflection criteria are defined as

$$d_y = \frac{E(\mathbf{y}_{s+n}) - E(\mathbf{y}_n)}{\sigma(\mathbf{y}_n)}, \quad d_w = \sqrt{K} d_y = \sqrt{K} \frac{E(\mathbf{y}_{s+n}) - E(\mathbf{y}_n)}{(E(\mathbf{y}_n^2) - E(\mathbf{y}_n)^2)^{1/2}}, \quad (\text{B-2})$$

where E denotes an ensemble average. The averages needed are given by

$$\begin{aligned} E(\mathbf{y}_n) &= \int du f(u) p_n(u), \\ E(\mathbf{y}_n^2) &= \int du f(u)^2 p_n(u), \\ E(\mathbf{y}_{s+n}) &= \int du f(u) p_{sn}(u). \end{aligned} \quad (\text{B-3})$$

To determine the probability density function (PDF) p_{sn} when signal and noise are present, a simplifying candidate signal PDF will be employed; this is not expected to be too critical for large K , when low input signal-to-noise ratios (SNRs) are relevant. In particular, the signal PDF is taken as flat over interval $(-v, v)$, where $v = \sqrt{3} \sigma_s$. There follows

$$p_{sn}(u) = \int dx p_s(x) p_n(u-x) = \frac{1}{2v} \int_{-v}^v dx p_n(u-x) = \frac{1}{2v} [c_n(u+v) - c_n(u-v)], \quad (\text{B-4})$$

where c_n is the noise CDF. Then, for use in equation (B-2), along with equation (B-3),

$$E(\mathbf{y}_{s+n}) = \int du f(u) \frac{1}{2v} [c_n(u+v) - c_n(u-v)], \quad v = \sqrt{3} \sigma_s, \quad (\text{B-5})$$

which can be numerically evaluated for the nonlinearity f of interest. Figure B-1 presents a program for this computation. The three noise PDFs are again Gaussian, sech, and fourth power. The nonlinearity of interest is the suboptimum processor given in equation (51) in the main report, namely,

$$f(u) = \min(u^2 - b^2, 0). \quad (\text{B-6})$$

The deflection d_w of output w of processor (B-1) for a Gaussian noise background is displayed in figure B-2. The abscissa r is the ratio b/σ of the saturation parameter to the noise standard deviation. As r increases, the deflection increases monotonically. This is consistent with the fact that the optimum processor in Gaussian noise is to let b tend to infinity, that is, no saturation at all. Alternatively, when interpreted as a hard limiter followed by an energy detector, the hard-limiting saturation point is allowed to tend to infinity, leading to the standard energy detector for a Gaussian noise background.

The deflection criterion for sech noise is given in figure B-3. For low input SNR, the best value of ratio r is 1; this is the value used for the ROCs in figures 18 through 20 in the main report. This best value was determined for the ROCs by simulation for several different values of r ; here, it has been deduced from the simpler deflection criterion. However, the plots in figure B-2 reveal that there is a rather broad maximum in the deflection, meaning that the choice of ratio r is not critical.

The deflection criterion for fourth-power noise is depicted in figure B-4. For low input SNR, the best ratio r is approximately 0.65, in agreement with the value used for the ROCs in figures 21 through 23 in the main report. The case of $r = 0.75$ (used in figure 24) has virtually the same deflection for small input SNR and is, in fact, slightly better than $r = 0.65$ as the SNR increases. However, the broad maxima of the deflection curves indicate that the exact choice of saturation point is not critical. The important feature of the nonlinearity is the saturation effect itself, which suppresses the heavy-tailed character of the non-Gaussian noises considered, and allows the weak input signal to make significant contribution to the output over many samples K .

```

clear all                % deflection_ahn
close all hidden
Nu=200;                  % Number of u increments
Na=200;                  % Number of a values
K=1000;                  % Number of time samples
Nb=11;                   % Number of SNRs
amax=4;                  % Abscissa range

q2=sqrt(2);
q3=sqrt(3);
qk=sqrt(K);
p2=pi/2;
a=[1:Na]/Na*amax;
d=zeros(Na,Nb);          % Deflection
for m=1:Na
    du=a(m)/Nu;
    u=[0:Nu]*du;          % 0 to a(m) Notice limited range.
    u2=u.^2;
    f=u2-a(m)^2;          % Limiter - squarer
    % pn=3/q2/pi./(1+2*u2)./(1+.5*u2);          % (F)
    % pn=.5*sech(p2*u);          % (S)
    pn=sqrt(.5/pi)*exp(-.5*u2);          % (G)
    yn=du*(2*sum(f.*pn)-f(1)*pn(1));
    y2n=du*(2*sum(f.*f.*pn)-f(1)^2*pn(1));
    sn=sqrt(y2n-yn^2);
    for n=1:Nb
        dB=-10+(n-1)*.5;
        sigs=10^(dB/20); % Signal standard deviation
        w=q3*sigs;        % Flat signal PDF
        % cnp=.5+(2*atan((u+w)*q2)-atan((u+w)/q2))/pi; % (F)
        % cnm=.5+(2*atan((u-w)*q2)-atan((u-w)/q2))/pi; % (F)
        % cnp=2/pi*atan(exp(p2*(u+w))); % (S)
        % cnm=2/pi*atan(exp(p2*(u-w))); % (S)
        cnp=phi(u+w); % (G)
        cnm=phi(u-w); % (G)
        psn=.5/w*(cnp-cnm);
        ysn=du*(2*sum(f.*psn)-f(1)*psn(1));
        d(m,n)=qk*(ysn-yn)/sn;
    end
end
end
figure(1), clf
plot(a,d,'k','linewidth',.7)
grid on, zoom on
orient tall

```

Figure B-1. Program for Deflection Criterion

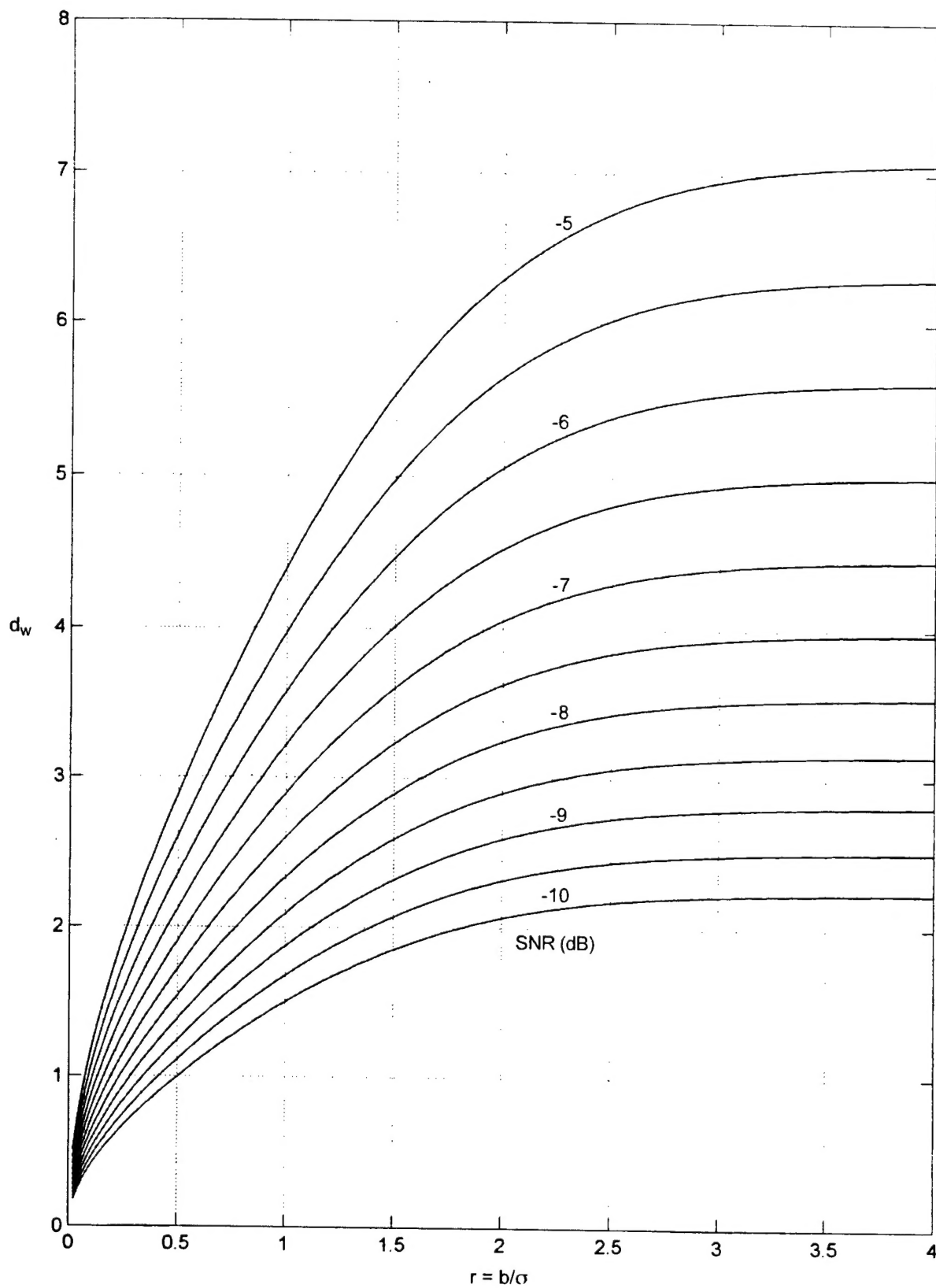


Figure B-2. Deflection for Gaussian Noise and Processor (B-6)

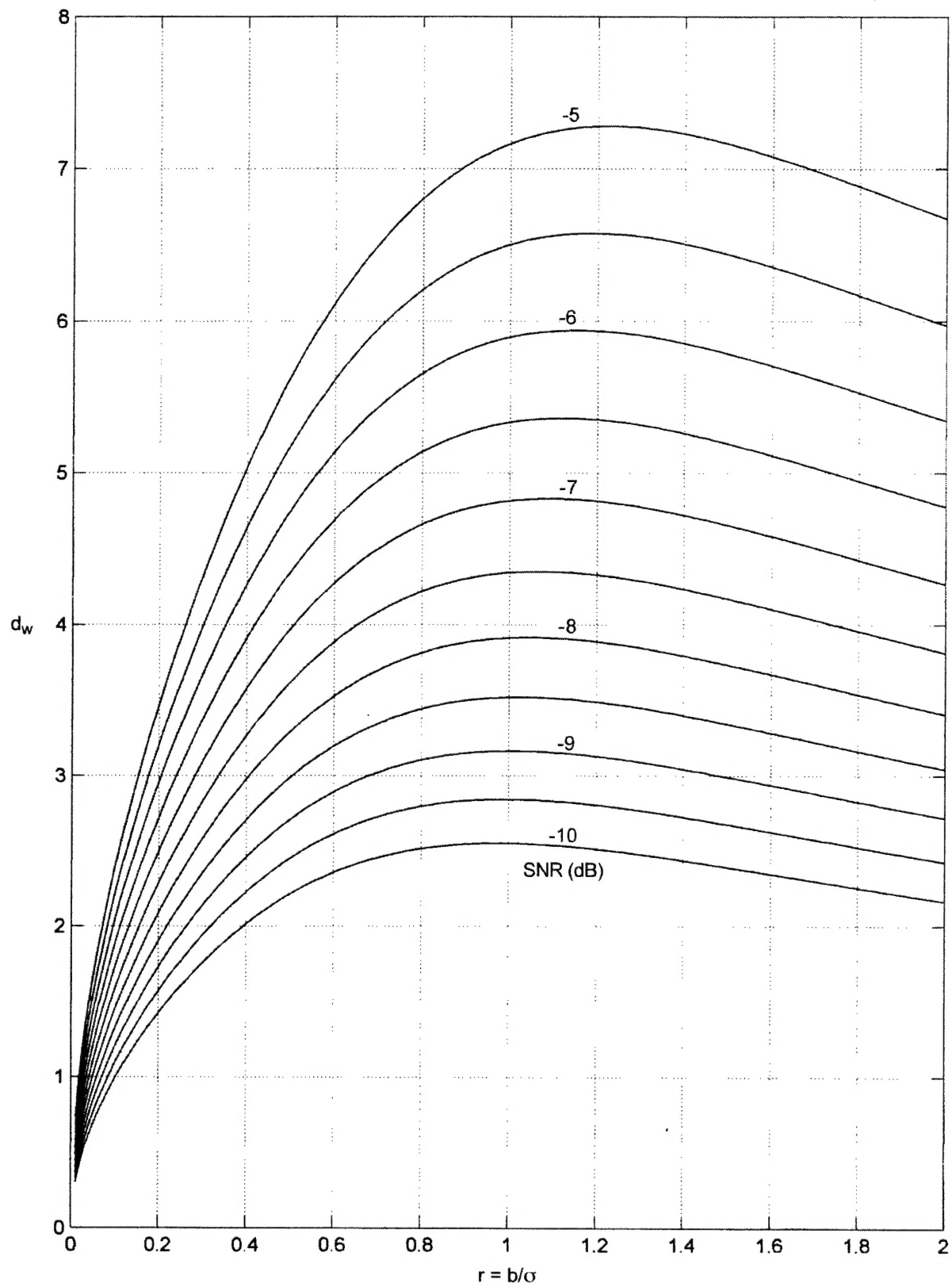


Figure B-3. Deflection for Sech Noise and Processor (B-6)

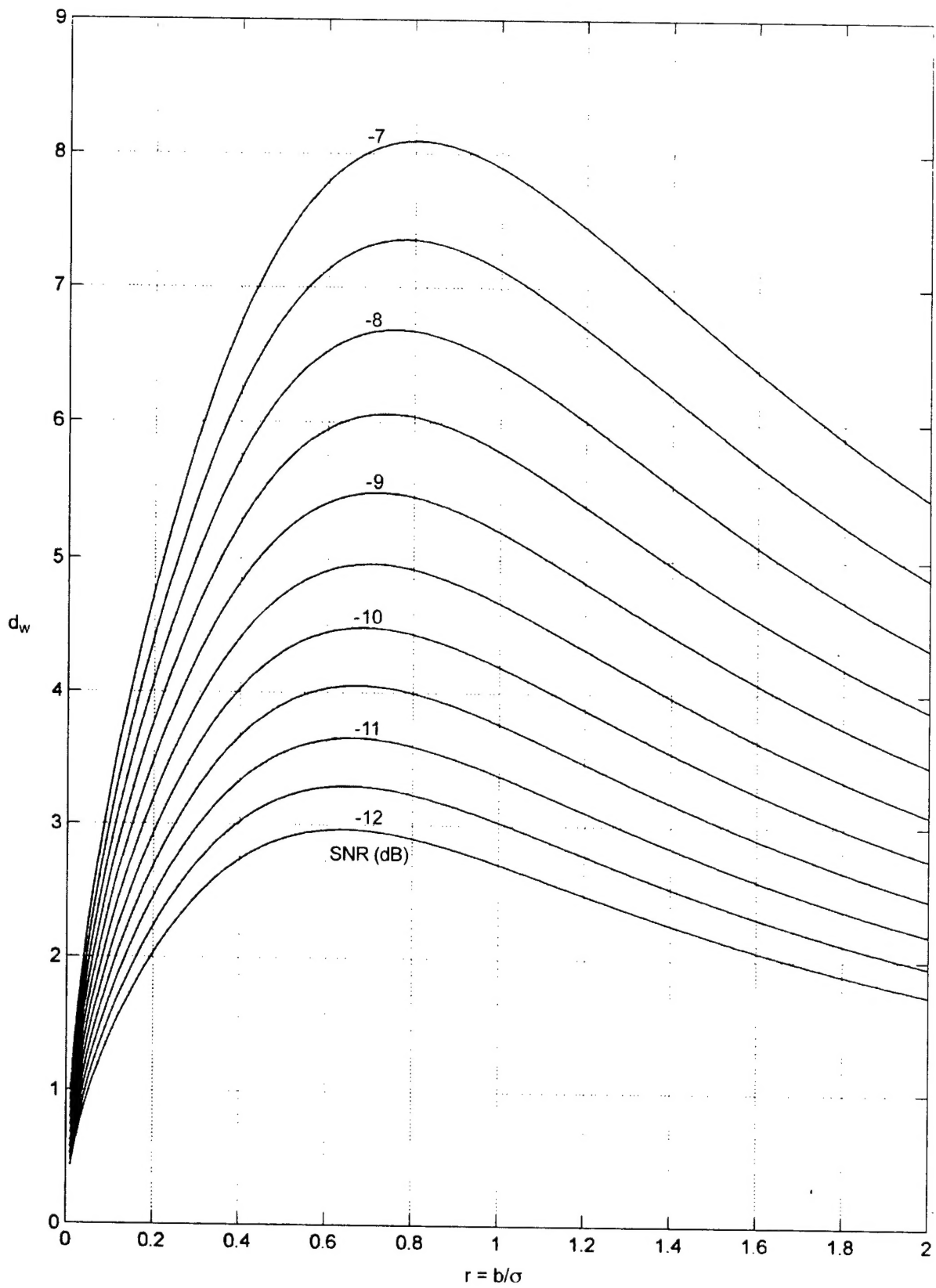


Figure B-4. Deflection for Fourth-Power Noise and Processor (B-6)

INITIAL DISTRIBUTION LIST

Addressee	No. of Copies
Office of Naval Research (ONR 32 (P. Abraham, B. Fitch, D. Johnson, F. Herr, J. Tague))	5
Naval Sea Systems Command (PEO-IWS 5 (R. Zarnich))	1
University of Connecticut (P. Willett)	1
University of Rhode Island (S. Kay)	1
Defense Technical Information Center	2
Center for Naval Analyses	1